Gut microbiota gate host exposure to metabolites from dietary Solanums

Catherine S. Liou[1], Mikhail Iakiviak[2], Jakub Rajniak[3], Pallavi P. Murugkar[2], Steven K. Higginbottom[4], Marissa Jasper[2], Michael A. Fischbach[2,3], Elizabeth S. Sattely[1,5]*

[1] Department of Chemical Engineering, Stanford University, Stanford, CA, USA
[2] Sarafan ChEM-H Institute, Stanford University, Stanford, CA, USA
[3] Department of Bioengineering, Stanford University, Stanford, CA, USA
[4] Department of Microbiology and Immunology, Stanford University School of Medicine, Stanford, CA, USA
[5] Howard Hughes Medical Institute, Stanford, CA, USA

*Corresponding author: sattely@stanford.edu

ABSTRACT

Dietary plants are molecularly rich but the fates of these compounds post-ingestion and their implications for human health are largely unknown. Here, we systematically characterized the major chemical contributions of widely consumed Solanum species (nightshades) to the human metabolome and established their mechanisms of production. Using untargeted metabolomics, we found a series of steroidal alkaloids resulting from tomatine, solanine, and chaconine that are dominant diet-derived compounds in systemic circulation following ingestion of potato and tomato. By comparing serum and tissue metabolomics of colonized and microbiome-depleted mice, we found that the gut microbiota metabolizes these compounds extensively, altering their absorption and gating host exposure to the diverse resulting metabolites. By screening metabolism with human stool samples, we established that steroidal glycoalkaloid metabolism varies inter-individually in a population. Further, using a collection of human commensal type strains, we found that a specific subset of strains in a community is responsible for steroidal glycoalkaloid metabolism, and chemical output of a community is determined by its strain-level composition. Microbial metabolism alters Solanum metabolite bioavailability and bioactivity in the context of acetylcholinesterase inhibition. The combination of dietary input and specific gut colonists dictate the composition of a variable component of the human metabolome. Our study provides insights into the molecular mechanisms of a diet-microbiome interaction and its effects on host physiology.

INTRODUCTION

Plants are sources of vast molecular diversity in diet, contributing not only carbohydrates, proteins, fats, and vitamins but also specialized small molecules. These secondary metabolites, produced by plants for defense, environmental stress tolerance, and nutrient acquisition, are estimated to be ingested in significant quantities of at least 50 milligrams per day[1,2] and have been associated with numerous pharmacological effects[3,4]. The immense chemical complexity of these plants outmatches our understanding of the major molecular inputs from diet, which obscures connections between dietary plant consumption and human health and disease states. Further exacerbating this challenge is metabolite transformation after ingestion, which vastly expands the array of diet-derived metabolites in the human metabolome.

In addition to host digestive processes, dietary compounds can be transformed by the commensal bacteria that reside in the gut. Gut microbiota-specific metabolism has an outsized impact on access to nutrients from diet[5] and we are only beginning to explore the specific molecular contributions by bacterial metabolism to the host metabolome[6,7]. Biotransformation by the gut microbiota can alter compound bioactivity and bioavailability; furthermore, microbiota-specific metabolism can vary inter-individually, resulting in divergent molecular exposures and health outcomes from a common dietary input[8,9]. Elucidation of bioactive compounds from diet, their transformation by gut microbiota, and their ultimate impacts on human health will not only expand our ability to take advantage of the benefits of dietary plants, but also provide valuable insight into the molecular interactions that exist at the interface of the plant, bacterial, and animal kingdoms.

Nightshades from the family Solanaceae, including potatoes, tomatoes, and eggplants, are of particular interest among dietary plants. Solanums are some of the most abundantly consumed plants in the United States[10] and are rich in specialized compounds studied in numerous physiological contexts, including carotenoids, steroidal glycoalkaloids, and flavonoids[11,12]. Diets rich in tomatoes and potatoes have been associated with different pharmacological effects; tomato ingestion, for example, has been shown to reduce serum LDL oxidation[13] and decrease the incidence of cardiovascular disease in a cohort of women[14]. However, the specific compounds that drive these pharmacological effects are still under active investigation.

In this study, we use dietary Solanums as a model to explore the major molecular inputs from a commonly consumed food, the role of gut microbiota in gating host exposure to these inputs, and the impacts of commensal-specific metabolism on compound bioavailability and

66 bioactivity. We used untargeted metabolomics in animal models and identified steroidal alkaloids
67 as the major diet-derived compounds in host circulation following Solanum ingestion. We mapped
68 the metabolic fates of dietary steroidal glycoalkaloids and reconstituted the production of these
69 metabolites *in vitro* and *ex vivo* using a combination of gut commensal strains and human liver
70 enzymes. These results reveal a paradigm where specific bacterial strains are responsible for key
71 steps in compound metabolism, yielding metabolite and bioactivity profiles unique to individual
72 community compositions. Biotransformation by the gut microbiota is a layer of metabolism that
73 can profoundly impact interactions between diet and the host and must be characterized to fully
74 understand the physiological effects of a dietary molecule.

75

76 **RESULTS**

77 **Major molecular inputs from dietary Solanums**

78 We focused on Solanums, including potatoes and tomatoes, as abundantly consumed
79 plants known to be rich in specialized compounds and began by exploring the major molecular
80 inputs derived from ingestion of these plants. We reasoned that an untargeted metabolomics
81 approach would enable unbiased identification of the compounds encountered post-ingestion that
82 may mediate the pharmacological effects associated with these plants. We used liquid
83 chromatography coupled to mass spectrometry (LC-MS) to profile serum from Swiss Webster
84 mice provided with *ad libitum* access to ripe Microtom tomatoes in addition to a standard diet for
85 15 days. To capture a broad range of molecule classes in serum, analyses were performed using
86 both hydrophilic interaction liquid chromatography (HILIC) for the retention of more polar
87 compounds and reverse phase chromatography for the retention of nonpolar compounds.
88 Untargeted metabolomics was used to identify tomato-associated compounds in systemic
89 circulation; mass features were filtered to identify those that significantly accumulated at least
90 three-fold higher in samples from mice receiving tomatoes than in mice that did not receive
91 tomatoes (**Fig S1A**). Many of these molecules were absent in the tomato supplement and are
92 likely derived from the metabolism of tomato compounds or endogenous mouse compounds
93 produced in response to tomato consumption (**Fig 1A**). We identified one such metabolite to be
94 trimethylamine N-oxide (TMAO), known to be produced by intestinal bacteria from dietary
95 trimethylamine containing precursors like choline, betaine, and carnitine[15]. Serum TMAO levels
96 were increased 2.5-fold by tomato consumption (**Fig S1B**), an unexpected result considering the
97 association of circulating TMAO with red meat consumption and increased risk for cardiovascular

98 disease[16]. These data highlight the strengths of an untargeted approach in identifying unexpected
99 compounds resulting from a dietary intervention.

100 When subjected to tandem mass spectrometry (MS/MS), fourteen of the 28 tomato-
101 associated compounds found in serum had mass fragmentation patterns characteristic of
102 steroidal alkaloids (SAs) (**Fig S1C**). Steroidal alkaloids are nitrogen containing compounds
103 derived from cholesterol and accumulate highly in Solanums as glycosides called steroidal
104 glycoalkaloids (SGAs). Solanums are known to biosynthesize species-specific SGAs with
105 structural variations in both the steroidal aglycone and the tetraose or triose glycone. Commercial
106 tomato cultivars accumulate the SGA tomatine, comprised of a tomatidine aglycone conjugated
107 to a lycotetraose moiety, which is converted *in planta* to esculeoside A during fruit ripening (**Fig**
108 **1B**). We found major SA compounds in serum following tomato consumption to include tomatidine
109 and esculeogenin A, the aglycones derived from tomatine and esculeoside A, respectively, as
110 well as other oxidized versions of SA aglycones (**Fig 1A**). Interestingly, despite the abundance of
111 SGA and the lack of detectable SA aglycones in the provided tomato, we observed primarily
112 aglycones accumulating in the serum. These results suggest that SGAs undergo significant
113 metabolism following consumption.

114

115 **Tomato steroidal glycoalkaloids are deglycosylated and further modified after ingestion**

116 To track the metabolic fates of SGAs independently of the other dietary components in
117 tomatoes, we next provided Swiss Webster mice with pure tomatine in drinking water. Reasoning
118 that metabolites may accumulate more highly in certain tissues than in systemic circulation, we
119 used untargeted metabolomics to characterize the major tomatine metabolites that are present in
120 animal tissues and therefore have the potential to interact with tissue-specific physiology. We
121 surveyed a panel of tissues for steroidal alkaloid content, including two tissues along the digestive
122 tract (colonic tissue and luminal contents from the cecum), another two that are first-pass tissues
123 for nutrient absorption (mesenteric lymph nodes (MLNs) for molecules transported by the
124 lymphatic system and liver for molecules transported by the portal vein), and kidney, based on
125 previous studies that have tracked tissue accumulation of SGAs from potato[17].

126 In addition to some of the SA metabolites previously detected in systemic circulation
127 following tomato ingestion, we were able to identify several aglycone metabolites that
128 accumulated highly in specific tissues (**Fig 1C**). Selected compounds were structurally
129 characterized through retention time and MS/MS spectrum matching to synthesized standards,

130 including tomatidine oxidized at the C3 alcohol to yield the ketone 3-oxotomatidine (**Fig S2A**) and
131 sulfated to form tomatidine 3-sulfate (**Fig S2B**). We also noted the accumulation of metabolites
132 putatively identified through MS/MS analyses to be C3-OH epimerized, acetylated, and doubly
133 hydroxylated analogues of tomatidine. These metabolites reveal that extensive structural
134 modifications of SGAs beyond deglycosylation occur following ingestion.

135 Because only SGAs were present in the dietary intervention, we next wanted to probe how
136 the abundant aglycones in serum and tissues were formed. Tomatine and many of the SA
137 aglycone metabolites were found primarily in the cecal contents and the colon (**Fig 1C**). A few
138 aglycones, however, including 3-oxotomatidine, hydroxytomatidine, and tomatidine sulfate were
139 also abundant in the liver. We hypothesized that these compounds could be formed by hepatic
140 metabolism. To test this hypothesis, we incubated human liver protein extracts with tomatine and
141 tomatidine. While human liver enzymes did not modify the parent SGA tomatine *in vitro*, we
142 observed formation of both tomatidine sulfate (**Fig S2C**) and hydroxytomatidine (**Fig S2D**) after
143 incubation with the aglycone tomatidine. While we could not detect any hepatic oxidation of
144 tomatidine to form 3-oxotomatidine, human liver enzymes were able to perform the reverse
145 reaction and non-selectively reduce synthesized 3-oxotomatidine to tomatidine and a putative
146 3αOH epimer of tomatidine (**Fig S2E**). Using human liver enzymes, we were able to recapitulate
147 the production of a few SA metabolites from tomatidine. Many of the major metabolic
148 transformations present in serum metabolites, however, including tomatine deglycosylation, were
149 not catalyzed by human liver enzymes *in vitro*. These data suggest that human liver enzymes
150 have a limited role in generating systemically circulating metabolites from SGAs.

151

152 **Potato steroidal glycoalkaloids from potato undergo similar metabolism as tomato SGAs**

153 To explore the major molecular inputs of other dietary Solanums and track their metabolic
154 fates, we provided Swiss Webster mice with a single dose of the potato SGA solanine, followed
155 by diet supplemented with 10% potato peel. Using a similar approach as for the tomato dietary
156 supplement, we performed untargeted metabolomics to identify the major diet-derived
157 metabolites that accumulated in systemic circulation (**Fig S3A**). We found that dietary intervention
158 with potatoes significantly increased serum levels of several compounds, including hippuric acid
159 (**Fig S3B**), potentially derived from metabolism of phenolic compounds abundant in potato[18]. The
160 majority of the compounds that accumulated in serum with potato consumption, however, had
161 MS/MS spectra characteristic of solanidine-based steroidal alkaloids (**Fig S3C**). These

162 metabolites included the major SGAs solanine and chaconine present in potato (**Fig 1B**), as well
163 as the corresponding aglycone solanidine. Reminiscent of the metabolic fates of tomatine, we
164 observed compounds produced by extensive structural modifications to the aglycone solanidine,
165 including hydroxylation, sulfation, and oxidation. We additionally observed hydrogenation of the
166 Δ5,6 double bond of solanidine to form 5α and 5β isomers of dihydrosolanidine, confirmed by
167 MS/MS spectrum and retention time matching to a synthetic standard (**Fig S4A**).

168 To investigate the biosynthetic origins of these serum metabolites, we next incubated
169 solanine, chaconine, and solanidine with human liver proteins *in vitro*. As was the case with the
170 tomato SGA, human liver proteins did not metabolize glycosides solanine and chaconine. We
171 recapitulated the formation of a subset of the modified aglycone metabolites observed in serum
172 by incubating liver proteins with solanidine, namely sulfated (**Fig S4B**) and hydroxylated (**Fig**
173 **S4C**) solanidine. However, other modified aglycone metabolites, including keto- and saturated
174 analogues of solanidine, were not produced. These data show that, like tomato SGAs, potato
175 SGAs undergo extensive modifications following deglycosylation, many of which are produced
176 independently of hepatic metabolism.

177 Taken together, we found that steroidal alkaloid aglycones represent a substantial portion
178 of the detectable diet-derived metabolites in systemic circulation following a meal of tomatoes and
179 potatoes. These data support other studies that have noted steroidal alkaloids and their
180 metabolites to be small molecule biomarkers characteristic of tomato consumption[19–21]. We further
181 characterized the SA metabolites observed *in vivo* to uncover previously uncharacterized
182 modifications that occur to SGAs following ingestion, including oxidations and hydrogenations.

183

184 **Gut microbiota gate the formation of steroidal alkaloid aglycones *in vivo***

185 As we could not detect aglycone formation from SGAs by human metabolic enzymes *in*
186 *vitro*, we next wanted to explore the mechanisms through which SGAs are deglycosylated *in vivo*.
187 Considering the relative abundance of SA aglycones within the digestive tract (**Fig 1C**) and the
188 established capabilities of gut commensals in polysaccharide hydrolysis[22], we hypothesized that
189 gut microbiota could play a role in mediating SGA metabolism. Fecal pellets from conventional
190 mice and mice treated with broad spectrum antibiotics[23] were incubated with exogenously added
191 tomatine. We observed formation of the aglycone tomatidine only in the feces of mice that had
192 not received antibiotics (**Fig S5A**), indicating that native murine commensals are capable of
193 tomatine deglycosylation.

194 In addition to gut microbiota, host digestive processes including acid hydrolysis in the
195 stomach and glycosidases in the intestine may also contribute to SGA deglycosylation. To assess
196 the contributions of gut microbiota towards SGA deglycosylation *in vivo*, we provided C57BL/6J
197 mice with diet supplemented with 10% tomato concurrently with antibiotics treatment. The
198 aglycone tomatidine was absent from serum (**Fig 2A**) and tissues (**Fig S5B**) in mice receiving
199 antibiotics treatment. Other modified aglycone metabolites, including 3-oxotomatidine and
200 tomatidine sulfate, were similarly depleted by antibiotics treatment (**Fig 2B**). Because the potato
201 SGAs are structurally distinct to tomatine, we also explored whether the gut microbiota is similarly
202 necessary for solanine and chaconine deglycosylation. C57BL/6J mice concurrently receiving
203 antibiotics and a diet containing potato peels were deficient in the aglycone solanidine, both in
204 systemic circulation (**Fig 2C**) and tissues that highly accumulated SGAs (**Fig S5C**). These
205 animals were also deficient in modified analogues of solanidine (**Fig S5D**). These data show that
206 SGA deglycosylation is performed primarily by gut microbiota and not host digestion. Additionally,
207 we observe that SGA deglycosylation by gut microbiota precede and gate the formation of the
208 extensive modified aglycone metabolites characterized *in vivo*.

209 To explore the relevance of this metabolism to humans, we analyzed urine from human
210 colectomy patients lacking an intact colon and therefore deficient in colonic microbiota[24]. Even
211 without a specified dietary intervention, we were able to detect potato SGAs solanine and
212 chaconine co-occurring in 8 out of 12 colectomy donors and 9 out of the 17 donors with intact
213 colons, indicative of recent potato consumption (**Fig S5E**). In donor samples that also contained
214 potato SGAs, the aglycone solanidine (**Fig 2D**) was largely depleted in colectomy patients
215 compared to donors with intact colons. We also detected solanidine metabolites modified by
216 hydroxylation, sulfation, and hydrogenation, transformations that we had observed in previous
217 mouse studies; these molecules were similarly depleted in colectomy patients relative to patients
218 with intact colons (**Fig S5F**). These data show not only that SA metabolites are found in systemic
219 circulation with presumed dietary exposure to Solanums, but that metabolism by gut microbiota
220 dictate SGA metabolism and host exposure to steroidal alkaloid aglycones.

221

222 **Inter-individual variation in *ex vivo* SGA metabolism by human stool samples**

223 A key implication of SGAs being metabolized exclusively by gut microbiota is the potential
224 variation in metabolism between individuals, with unique bacterial communities generating distinct
225 metabolite profiles from a common molecular input. Having established the necessity of gut

226 microbiota in metabolizing SGAs, we next explored how these compounds might be metabolized
227 differently between individuals. We began by identifying the major compounds produced from
228 SGAs by complex human gut microbial communities. Thirty human stool samples[25] were
229 incubated *ex vivo* with the major SGAs from dietary Solanums and assayed for product formation
230 by LC-MS. In addition to potato and tomato SGAs, we also included SGAs from eggplant,
231 solamargine and solasodine, which share a solasodine aglycone but differ in their glycone
232 moieties. MS fragmentation was used to identify mass features containing characteristic steroidal
233 alkaloid substructures (**Fig S6A**). Using this approach, we found compounds that had not been
234 previously observed in our analyses of mouse samples, including putative phosphoethanolamine
235 conjugation to the aglycones tomatidine and solasodine (**Fig S6B**).

236 Comparing glycoalkaloid conversion by different human donor samples, we observed
237 significant inter-individual differences in SGA deglycosylation, with some samples extensively
238 metabolizing SGAs and others inactive (**Fig 3A**). SGA metabolism also appeared to correlate with
239 identity of the glycone. Solanine and the eggplant SGA solasonine share the same solatriose
240 glycone and were metabolized by a similar subset of samples. In the same manner, another
241 subset of donors was able to metabolize chaconine and the eggplant SGA solamargine, which
242 share a chacotriose sugar.

243 We further tested the ability of donor samples to metabolize steroidal alkaloid aglycones.
244 In addition to variation in SGA deglycosylation, we also observed inter-individual variation in the
245 major modifications made to exogenously added aglycone. Hydrogenation of Δ5,6 aglycones
246 solanidine and solasodine was previously observed in mice following potato consumption (**Fig**
247 **S5D**) and occurred only in two out of the 30 human stool samples surveyed (**Fig 3B**). More
248 common modifications included phosphoethanolamine conjugation to tomatidine and solasodine,
249 as well as oxidation and sulfation of all three aglycones surveyed. The variation in the abundance
250 and identity of metabolites produced *ex vivo* by different human stool samples indicate that, from
251 a common input of dietary Solanums, individuals may be exposed to different compounds
252 depending on compositions of gut microbial communities.

253 We noted that some samples that did not metabolize SGAs were nonetheless active on
254 the corresponding aglycone. For example, sample 26 did not significantly metabolize either
255 solanine or solasonine, but still produced abundant sulfonated aglycone when incubated directly
256 with solanidine and solasodine (**Fig S7**), respectively. These results suggest that SGAs may be
257 metabolized cooperatively by the gut microbiota, with different strains responsible for
258 deglycosylation and aglycone modification.

259

260 **Cooperative metabolism by human commensal type strains**

261 Having noted significant variation in SGA metabolism by human stool samples, we sought
262 to identify specific human commensal strains involved in these metabolic steps. We individually
263 cultured 116 human commensal type strains, selected to represent strains that are abundant and
264 prevalent in a Western microbiome[26], in rich medium containing potato and tomato SGAs and
265 assayed for compound metabolism using LC-MS. Following incubation with tomatine, aglycones
266 were produced by only a few strains out of those surveyed, including *Roseburia intestinalis* L1-
267 82, *Bacteroides uniformis* ATCC 8492, and strains from the genus *Parabacteroides* (**Fig 4**).
268 Among these strains, *Parabacteroides distasonis* ATCC 8503 was notable for being able to
269 metabolize all three SGAs surveyed. Generally, however, the capacity of a strain to deglycosylate
270 one SGA did not guarantee the metabolism of other SGAs. *Ruminococcus gnavus* ATCC 29149,
271 for example, was able to hydrolyze chaconine but not solanine, despite the identical aglycone
272 moiety. These data show that SGA deglycosylation is a substrate-specific transformation
273 performed by only select strains in a community.

274 To circumvent the necessity for SGA deglycosylation and directly assay for aglycone
275 modification, we additionally incubated the commensal strains directly with aglycones tomatidine
276 and solanidine. Bacteroidetes were found to be broadly active on these compounds to generate
277 the same sulfated and phosphoethanolamine-conjugated metabolites previously produced by
278 human stool. Some of the strains that were active on SGAs were also capable of modifying the
279 resulting aglycone; *Bacteroides uniformis* ATCC 8492 produced sulfonated and
280 phosphoethanolamine-conjugated compounds following incubation with both tomatine and
281 tomatidine. However, SGA deglycosylation appeared to be generally independent of aglycone
282 modification, with different subsets of strains active on the aglycone and the corresponding
283 glycoside.

284 Since SGA deglycosylation and aglycone modification are generally carried out by
285 different strains, we hypothesized that SGAs may be metabolized cooperatively in a community
286 context, reliant on a subset of strains to liberate the aglycone before further modification by other
287 members of the community. We explored this possibility by incubating cocultures of defined
288 composition with tomatine in rich medium. Six *Bacteroides* strains were selected for their ability
289 to modify tomatidine but not deglycosylate tomatine (**Fig S8**). Inclusion of either *Roseburia*
290 *intestinalis* LI-82 or *Roseburia inulinivorans* DSM 16841, strains capable of deglycosylation but

291 not aglycone modification, in the coculture enabled production of sulfonated,
292 phosphoethanolamine-conjugated, and acetylated tomatidine. From these results, we show that,
293 despite their relative hydrophobicity, steroidal alkaloid aglycones are exchanged as intermediates
294 between bacterial strains in a community. Furthermore, we see that the major compounds derived
295 from SGAs *in vitro* can be manipulated by the strains present in a community. These results
296 support our findings that that inter-individual differences in microbiome composition (**Fig 3**) drive
297 divergent host exposure to SA metabolites.

298

299 **SGA metabolism by gut microbiota dictates compound bioavailability and bioactivity**

300 Having established that SGAs are major dietary inputs from dietary Solanums and that gut
301 microbiota dictate the metabolic fates of dietary SGAs, we next explored the consequences of
302 this metabolism on host physiology. As hydrolysis of the glycone by gut microbiota significantly
303 impact physiochemical properties like solubility and molecular size, we began by investigating the
304 impact of SGA deglycosylation on compound bioavailability. We used a Caco-2 human colonic
305 cell monolayer as a model for compound transport across the intestinal enterocyte barrier[27].
306 Potato SAs solanine, chaconine, and solanidine were added to the apical side of the monolayer
307 representing the intestinal lumen. Following incubation, compound transport across the
308 monolayer was determined using LC-MS. While the SGAs solanine and chaconine primarily
309 remained on the apical side, the majority of the aglycone solanidine was observed to accumulate
310 on the basolateral side, indicating that solanidine is better transported across the epithelium than
311 SGAs (**Fig S9A**). We next reproduced these differences in bioavailability *in vivo* in mice fed
312 potatoes concurrently with antibiotics treatment. The total quantity of SGA-derived compounds
313 absorbed into systemic circulation was estimated as the sum of serum SGAs and tracked
314 agylcones. We found that animals with intact gut microbiota had significantly higher
315 concentrations of total SGA-derived metabolites in serum relative to mice that had been treated
316 with antibiotics, with aglycones representing the majority of these compounds (**Fig 5A**). Taken
317 together, these data show that metabolism of SGAs by the gut microbiota convert SGAs to a
318 better absorbed form and influence circulating concentrations of these specialized steroidal
319 alkaloid compounds in the host.

320 Having noted differences in bioavailability resulting from SGA metabolism, we next
321 explored the impact of gut microbiota-mediated SGA metabolism on compound biological activity.
322 SAs have been shown to have numerous effects on host physiology, including anti-inflammation[28]

323 and chemoprevention through cytotoxicity in cancer cell lines[29–31]. We began by exploring the
324 impact of deglycosylation on SGA cytotoxicity *in vitro*. We treated the human colon cancer cell
325 line Caco-2 with potato SGAs solanine and chaconine and observed concentration-dependent
326 loss of cell viability. In contrast, the aglycone solanidine had a negligible impact on cell viability
327 (**Fig S9B**). A similar connection between glycosylation and *in vitro* toxicity was observed for the
328 tomato SGA tomatine and the aglycone tomatidine (**Fig S9C**)[31]. These data suggest that SGA
329 deglycosylation by gut microbiota inactivates the toxic potential of these compounds.

330 In addition to cytotoxicity and uniquely among the dietary SGAs, the potato SGAs solanine
331 and chaconine are established cholinergic toxins in humans, capable of inhibiting the two
332 cholinesterases that terminate acetylcholine (ACh) neurotransmission[32,33] and implicated in
333 poisonings caused by the ingestion of improperly stored potatoes[34]. Considering the established
334 interactions between potato SGAs and these physiologically essential cholinesterases, we next
335 explored the effects of gut microbiota-mediated SGA metabolism on ACh hydrolysis.
336 Recombinant human acetylcholinesterase (AChE) and butyrylcholinesterase (BChE) were
337 treated with solanine, chaconine, and solanidine, with enzyme activity measured by tracking
338 hydrolysis of substrate mimics acetylthiocholine and butyrylthiocholine, respectively[35]. The SGAs
339 solanine and chaconine inhibited acetylthiocholine hydrolysis relative to a vehicle treated control
340 in a dose-dependent manner while the aglycone solanidine did not significantly impact AChE
341 activity at concentrations up to 100 μM (**Fig 5B)**. While AChE activity was not impacted at the
342 concentrations tested, solanidine did inhibit BChE activity to similar extents as did the SGAs (**Fig**
343 **S9D**). These results show that deglycosylation of potato SGAs solanine and chaconine to the
344 aglycone solanidine alleviates AChE inhibition but not BChE inhibition by these compounds.
345 Furthermore, we showed with physiologically relevant dietary interventions that SGAs can
346 accumulate to micromolar quantities gastrointestinal tissue. In animals concurrently receiving 5%
347 potato peel in diet with antibiotics, colonic levels of SGAs accumulated to 2.98 ± 0.38 pmol/mg
348 fresh weight tissue (**Fig S5C**), concentrations which corresponded to about 40% inhibition of
349 AChE activity *in vitro*.

350 In addition to its role in the central nervous system, ACh is a key neurotransmitter in the
351 enteric nervous system[36]. Because AChE and BChE can both contribute to ACh hydrolysis in the
352 gastrointestinal tract, we aimed to investigate the effects of SGA metabolites on a physiological
353 mix of cholinesterases. We chose to focus on the colon as the primary tissue of interest, as SGAs
354 are present in high concentrations in the gastrointestinal tract and extensively metabolized by
355 colonic microbiota. Protein homogenates were prepared from human colonic tissue samples and

356 Caco-2 colonic epithelial cells. We incubated these samples with equal concentrations of
357 solanine, chaconine, and solanidine, and assayed for acetylthiocholine hydrolysis. Treatment of
358 both Caco-2 and colon tissue homogenates with SGAs strongly inhibited ACh hydrolysis (**Fig 5C**).
359 In contrast, treatment of tissue homogenates with an equal concentration of the aglycone
360 solanidine only slightly inhibited ACh hydrolysis; in Caco-2 lysates, ACh hydrolysis was
361 completely unaffected by solanidine. The observed differences in the effect of solanidine on ACh
362 hydrolysis by Caco-2 lysates and colonic tissue may result from differences in relative BChE
363 quantities. Indeed, treatment of these samples with the BChE selective inhibitor iso-OMPA
364 showed more significant contributions of BChE towards ACh hydrolysis in colonic tissue than in
365 Caco-2 (**Fig S9E**). The modest inhibition of ACh hydrolysis in colonic tissue by solanidine was
366 rescued by concurrent treatment with iso-OMPA, while ACh inhibition by the glycosides solanidine
367 and chaconine remained unaffected (**Fig S9F**). These data show that potato SGAs inhibit overall
368 ACh hydrolysis in relevant host tissues and deglycosylation of these compounds alleviates this
369 inhibition.

370 To directly connect microbial SGA metabolism to the activity of host AChE, we used spent
371 media from individual human stool samples incubated with solanine to modulate AChE activity.
372 These donor samples were selected to have a range of solanine metabolism (**Fig 3A**), including
373 samples inactive on solanine and samples that deglycosylated solanine. Solanine metabolism by
374 different donor samples resulted in significant differences in ACh hydrolysis. Media from inactive
375 stool samples inhibited AChE while stool samples with extensive aglycone production showing
376 only slight AChE inhibition (**Fig 5C**). These data show that the inter-individual differences that
377 exist in microbiota-mediated SGA metabolism can translate to varying levels of host AChE
378 inhibition *ex vivo*. Taken together, our mapping of the metabolic fates of dietary SGAs revealed
379 the crucial role of gut microbiota in controlling host exposure to and host enzyme interactions with
380 these compounds.

381

382 **DISCUSSION**

383 Beyond steroidal glycoalkaloids from Solanums, other saponins of plant origin have been
384 shown to undergo gut microbiome-mediated deglycosylation. Ginsenosides from the root of
385 *Panax ginseng* were found to be deglycosylated to the protopanaxadiol aglycone, mediated by
386 *Bacteroides*, *Bifidobacterium*, *Fusobacterium*, and *Prevotella* strains[37]. In contrast to our
387 observations with SGA metabolism, however, ginsenosides do not appear to be solely dependent

388 on the gut microbiome for metabolism and are also hydrolyzed by host digestive processes[38].
389 Beyond saponins, other dietary plant glycosides are also known to be metabolized by the gut
390 microbiota. A notable example are flavonoids, which undergo microbiota-mediated
391 deglycosylation and extensive metabolism to form phloroglucinol, catechol, and equol, among
392 other products[39]. The ability of broad specificity host glycosidases to metabolize flavonoids varies
393 with the identity and linkage of the glycone moiety[40]. In contrast to many plant glycosides
394 encountered in the diet and potentially resulting from the complexity of the glycone moieties, we
395 find SGAs from Solanums to be unusually resistant to hydrolysis by host enzymes and digestion.
396 These results support previous observations that tomatine is stable to incubation in acidic
397 conditions at 37°C[41], and is reminiscent of nondigestible dietary fibers that are fermented by gut
398 commensals[42].

399 In this work, we have established a direct link between human gut commensals and SGA
400 metabolism, both in the context of complex communities from human stool and with individual
401 type strains in culture. Under the conditions used to culture the commensal type strains, we found
402 that SGA metabolism is performed by a small subset of the strains in a representative community.
403 While Solanum plant pathogens are known to deglycosylate SGAs (**Supplemental Discussion**)
404 and clearly benefit from deactivation of these plant defense compounds, the motivation of gut
405 commensals to deglycosylate SGAs is less apparent. One possible motive for commensal
406 metabolism of SGAs is access to the liberated sugars as a competitive advantage in a community
407 context; gut commensals are known to harvest sugars from plant glycosides for use as carbon
408 sources[43]. Regardless, identification of the strains involved in SGA deglycosylation enables
409 further investigation into the ecological and genetic bases of this metabolism, understanding of
410 the prevalence of this metabolism across human populations, and the rational design of synthetic
411 communities that produce a desired metabolite output[44].

412 Though SA aglycones are formed from gut microbiota-mediated deglycosylation of dietary
413 SGAs, we have found that they are transient intermediates both *in vivo* and in the context of a
414 synthetic bacterial community. Our efforts to characterize the metabolite fates of SGAs have led
415 to the identification of aglycones that are modified further by hydroxylation, sulfation, 3OH
416 oxidation, Δ5,6 saturation, and phosphoethanolamine conjugation. There is rich biology
417 associated with each of these transformations promoted by subsets of gut microbial communities
418 (**Supplemental Discussion**). A major transformation that we observed in both mouse systemic
419 circulation and in human urine involved hydrogenation of the Δ5,6 double bond of the potato
420 aglycone solanidine. A previous report of such a compound noted its formation in bovine rumen

421 fluid from a solanine input[45]. More broadly, however, this reduction is reminiscent of gut
422 microbiota-mediated hydrogenation of cholesterol to coprostanol. Bacteria identified to be
423 coprostanol producers include *Bacteroides* sp. D8[46] and strains from the genus *Eubacterium*[47,48].
424 In human gut communities, the cholesterol dehydrogenase ismA from uncultured Clostridia has
425 been implicated in coprostanol formation[49]. Despite the analogous transformations observed for
426 solanidine and cholesterol, however, we observed solanidine hydrogenation to be performed by
427 Bacteroidetes, including *Alistipes finegoldii* DSM 17242 (**Fig 4**). A BLAST search revealed no
428 close homologs for *ismA* homologs in the solanidine reducing strains. As such, we hypothesize
429 that solanidine hydrogenation proceeds by a route distinct to the one identified for coprostanol
430 formation.

431 Crucially, metabolism of dietary SGAs by gut microbiota can transform the bioavailability
432 and bioactivity of these compounds in the host. Potato SGAs are AChE inhibitors, a class of
433 compound associated with drastic pharmacological and toxicological impacts. Systemic AChE
434 inhibition, including irreversible enzyme inhibition by sarin and organophosphates, can be lethal
435 due to the local accumulation of ACh and continued stimulation of vital nervous processes.
436 However, reversible and tissue specific AChE inhibition is a clinical strategy for the treatment of
437 Alzheimer's disease[50], glaucoma[51], and post-operative ileus[52]. The evidence for the toxicological
438 impacts of potato SGAs is extensive; improper storage of potatoes can result in overaccumulation
439 of SGAs and has led to numerous reports of SGA-induced poisonings[34], with an estimated toxic
440 dose of 2-5 mg/kg body weight in humans[53]. Acute symptoms of SGA toxicity commonly involve
441 nausea, vomiting and diarrhea[54], indicative of effects local to the gastrointestinal tract. Moreover,
442 treatment with the acetylcholine receptor inhibitor atropine was found to alleviate toxicity following
443 of solanine administration in mice[55], suggestive of a role for cholinesterase inhibition in mediating
444 toxicity. We show in this study that the gut microbiota alleviates the AChE inhibitory properties of
445 potato SGAs solanine and chaconine by deglycosylating the compounds to a non-inhibitory form
446 (**Fig 5C**). We hypothesize that gut microbiota can significantly diminish the toxicity of these
447 compounds *in vivo*.

448 In the colon where we found SGAs to significantly accumulate, acetylcholine is additionally
449 a key regulator of multiple processes including chloride secretion[56], epithelial proliferation[57], fluid
450 secretion[58], and intestinal propulsion[59]. Considering the role of ACh in these diverse physiological
451 processes, we suspect that AChE inhibition by SGAs may impact colonic physiology through a
452 myriad of mechanisms beyond overt toxicity. While there is still much to be investigated regarding
453 the contributions of the gut microbiota to mitigating the symptoms of SGA exposure, we show that

454 gut microbial metabolism can significantly deplete SGA levels in the colon *in vivo* following a
455 potato dietary intervention (**Fig S5C**). Furthermore, variation in the abilities of individual microbiota
456 to deglycosylate potato SGAs (**Fig 3A**) can lead to interindividual differences in host exposure to
457 these bioactive SGAs. Finally, these results emphasize the need for considering gut microbiota
458 in future studies investigating the physiological impacts of SGAs.

459 In addition to the depletion of bioactive SGAs by microbiota-mediated deglycosylation, the
460 products of this metabolism may have distinct physiological effects. For example, dietary
461 intervention with the aglycone tomatidine was found to increase mTORC1 signaling in mice,
462 resulting in increased skeletal muscle hypertrophy and decreased adiposity[60]. Further modified
463 versions of steroidal aglycones produced by host or bacterial metabolism may also result in
464 differential activity relative to the unmodified aglycone. For example, modification of the bile acid
465 lithocholic acid by oxidation at the C3 alcohol, a transformation that we also observed with
466 tomatidine and solanidine, enabled binding of the compound to host RORγt receptors and
467 resulted in inhibition of T_H17 cell differentiation[61].

468 Taken together, our characterization of the metabolic fates of SGAs and the role of
469 microbiota in determining host exposure lays a foundation towards a more complete
470 understanding of the effects that this abundant class of dietary plant metabolites may have on
471 host physiology.

472

473 **MATERIALS AND METHODS**

474 **Chemicals**

475 Steroidal alkaloid compounds were acquired from commercial sources: tomatine (Tokyo
476 Chemical Industry), tomatidine (Cayman Chemical Company), solanine (Sigma Aldrich),
477 chaconine (Sigma Aldrich), solanidine (Carbosynth), solamargine (MedChemExpress),
478 solasonine (MedChemExpress), solasodine (Santa Cruz Biotechnology). All steroidal alkaloid
479 compounds were prepared as 10 mM stocks in vehicle. Steroidal glycoalkaloids were dissolved
480 in dimethylsulfoxide (DMSO). Tomatidine and solasodine were dissolved in methanol and
481 solanidine was dissolved in ethanol. Other chemical standards were acquired as follows:
482 trimethylamine N-oxide (Cayman Chemical Company), trigonelline chloride (Cayman Chemical
483 Company), and hippuric acid (Sigma Aldrich).

484

485 **Mouse Studies**

486 Animal studies were performed under a protocol approved by the Stanford University
487 Institutional Animal Care and Use Committee. For all studies, groups of five 6-8 week old female
488 mice were used and allowed to acclimate for a week before any treatment.

489 *Ad libitum* fresh tomato feeding
490 Swiss Webster mice (Taconic) were fed *ad libitum* with AIN93G diet (Dyets, Inc). Three days
491 following the start of AIN93G diet, 40 g of red ripe Microtom tomatoes were provided daily
492 alongside diet for each cage of five mice for 15 days, with uneaten tomatoes removed daily
493 before replenishing with fresh tomatoes. The quantities of tomatine and esculeoside A in the
494 provided tomatoes were determined by liquid chromatography-mass spectrometry (LC-MS) as
495 described below to be about 0.72 μmol/g fresh weight 16sculeoside A and 0.074 μmol/g fresh
496 weight tomatine. Molar quantities of both compounds were estimated using a commercial
497 tomatine standard (Tokyo Chemical Industry). Mice were sacrificed by CO_2 asphyxiation 24
498 hours following the final provision of tomatoes. Blood was collected by cardiac puncture into
499 Microtainer SST tubes (BD) and serum harvested. All samples were frozen in liquid nitrogen
500 and stored at -80°C until analysis.

501 Pure tomatine feeding
502 Swiss Webster mice (Taconic) were fed *ad libitum* with AIN93G diet (Dyets, Inc). Three days
503 following the start of AIN93G diet, mice were provided with 15 μM pure tomatine in drinking
504 water. Drinking water was sterile filtered and refreshed every 2 to 4 days for 15 days, after
505 which mice were sacrificed by CO_2 asphyxiation and serum, cecal contents, colon, liver,
506 kidneys, and mesenteric lymph nodes (MLNs) were harvested. Samples were frozen in liquid
507 nitrogen and stored at -80°C until analysis.

508 Potato feeding
509 Swiss Webster mice (Taconic) were fed *ad libitum* with AIN93G diet (Dyets, Inc). One week
510 following the start of AIN93G diet, mice were dosed with 0.5 μmol solanine per mouse by oral
511 gavage. Two days following this single dose, mice were provided with 10% w/w potato peels
512 incorporated into AIN93G diet. Potato-supplemented diet was prepared by autoclaving peels
513 from Yukon Gold potatoes at 121°C for 30 minutes, lyophilizing to dryness, and homogenizing
514 using a blender to generate dry powder. Potato peel powder was mixed into powdered AIN93G
515 diet (Dyets, Inc) at 10% w/w, moistened with water to pellet, and then lyophilized to dryness.
516 The quantity of solanine and chaconine in the provided potato-supplemented diet was

517 determined by LC-MS as described below to be about 0.4 μmol/g diet chaconine and 0.11
518 μmol/g diet solanine. Mice that did not receive potato diet instead received similarly pelleted
519 AIN93G. After one day of potato-supplemented diet, mice were sacrificed by CO_2 asphyxiation
520 and serum was collected. Samples were frozen in liquid nitrogen and stored at -80°C until
521 analysis.

522 Antibiotics treatment for *ex vivo* feces metabolism

523 Swiss Webster mice (Taconic) were fed ad libitum with AIN93G diet (Dyets, Inc). Three days
524 following the start of AIN93G diet, mice received five consecutive daily doses of 10 mg each
525 ampicillin, vancomycin, metronidazole, and neomycin by oral gavage[62]. Each mouse received
526 0.25 mL of a combined stock of 40 g/L of each antibiotic prepared in phosphate buffered saline
527 (PBS, pH 7.2). Mice not treated with antibiotics instead received 0.25 mL of PBS by oral
528 gavage. Following five daily doses of antibiotics by oral gavage, antibiotics were provided *ad*
529 *libitum* in drinking water for three days: ampicillin (1 g/L), vancomycin (0.5 g/L), neomycin (1
530 g/L), and metronidazole (1 g/L)[23]. Feces were collected into sterile tubes and processed as
531 described below.

532 Concurrent antibiotics treatment and dietary intervention

533 C57BL/6J mice (Jackson Laboratory) were fed *ad libitum* with AIN93G diet (Dyets, Inc). One
534 week following the start of AIN93G diet, antibiotics were provided *ad libitum* in drinking water for
535 the duration of the study: ampicillin (1 g/L), vancomycin (0.5 g/L), neomycin (1 g/L), and
536 metronidazole (1 g/L). Antibiotics were refreshed every 3-4 days. Six days following the start of
537 antibiotics treatment, mice were provided potato-supplemented diet (5% dry weight), prepared
538 as described above. Another set of mice was provided tomato-supplemented diet (10% dry
539 weight) seventeen days following the start of antibiotics treatment. Sugar plum tomatoes were
540 incorporated into AIN93G diet as described for potato supplemented diet above, but surface-
541 sterilized with 70% ethanol instead of autoclaved. Animals received potato supplemented diet
542 for 8 days or tomato supplemented diet for 7 days, and were then sacrificed by CO_2
543 asphyxiation. Serum, colon, livers, cecal contents, kidneys, and MLNs were collected and
544 frozen in liquid nitrogen and stored at -80°C until analysis.

545 Sample preparation for LC-MS

546 Harvested tissues were lyophilized to dryness and then homogenized using a ball mill
547 homogenizer (Retsch). Homogenized tissues were extracted with a fixed volume of 2:1:1
548 acetonitrile (MeCN):methanol(MeOH):water(H_2O) per dry mass tissue, vortexed to mix, and then
549 centrifuged at 18,000 *g* for 10 minutes. The resulting supernatant was optionally diluted (for

550 cecal content samples) and then filtered through a 0.45 µm PTFE for analysis by LC-MS, as
551 described below.

552 Serum samples were thawed and proteins precipitated by the addition of three volumes of ice
553 chilled 3:1 MeCN:MeOH. Samples were incubated on ice for 10 minutes, and then centrifuged
554 at 18,000 *g* for 10 minutes at 4°C. To concentrate the sample, supernatant was transferred to a
555 new microfuge tube, flash-frozen in liquid nitrogen, and lyophilized to dryness. Dried samples
556 were resuspended in 2:1:1 MeCN:MeOH:H_2O to the original volume of serum and filtered
557 through a 0.45 µm PTFE for analysis by LC-MS.

558

559 **Steroidal alkaloid metabolism by human liver enzymes**

560 To assay for metabolism of steroidal alkaloids by human liver enzymes, 1 mg/mL of liver S9
561 proteins from pooled human donors (Sekisui XenoTech) was incubated in PBS pH 7.4,
562 supplemented with 25 µM tomatine, tomatidine, solanine, chaconine, or solanidine. Samples
563 were incubated at 37°C for 5 minutes. Metabolism was initiated by the addition of cofactors
564 required for metabolic reactions and supplied as two separate mixtures: 1) 1 mM glutathione, 2
565 mM NADPH, and 0.5 mM acetyl-CoA, and 2) 200 µM 3'-phosphoadenosine-5'-phosphosulfate
566 (PAPS), 500 µM uridine diphosphate glucuronic acid (UDPGA), 25 µg/L alamethicin, 2 mM
567 magnesium chloride, and 2 mM NADPH. Each reaction was prepared in duplicate, with one set
568 immediately quenched by the addition of three volumes of cold 3:1 MeCN:MeOH. The other set
569 of reactions was incubated at 37°C for 60-90 minutes and then quenched as described above.
570 Quenched samples were stored at -80°C overnight, thawed, and centrifuged at 18,000 *g* for 10
571 minutes. The resulting supernatant was collected and filtered through 0.45 µm PTFE for
572 analysis by LC-MS.

573

574 **Synthesis of standards for steroidal alkaloid metabolites**

575 <u>3-oxotomatidine</u>
576 Synthesis of 3-oxotomatidine was adapted from previous reports[63]. Tomatidine hydrochloride
577 was dissolved in dichloromethane (DCM). Three molar equivalents of Dess-Martin periodinane
578 (DMP, Alfa Aesar) was added and the mixture was stirred at room temperature overnight. The
579 reaction was quenched with one volume of 0.8 M sodium thiosulfate and saturated sodium
580 bicarbonate, stirred at room temperature for 1 hour, and then extracted with three subsequent

581 volumes of DCM. The organic layers were combined and dried on anhydrous calcium sulfate.
582 LC-MS analysis of the reaction products at this stage generally revealed a conversion of about
583 50%. To improve substrate conversion, three equivalents of DMP were again added to this
584 mixture and the work repeated as described above. LC-MS analysis of the crude reaction after a
585 second round of reaction generally showed little detectable remaining unreacted tomatidine.

586 To isolate the produced 3-oxotomatidine, crude reaction products in DCM were dried down,
587 resuspended in a small volume of N,N-dimethylformamide (DMF), and separated by reversed
588 phase chromatography using a 100Å, 30 µm, 12 g Sfär C18 D Duo column (Biotage). Water
589 with 0.1% (v/v) formic acid and acetonitrile with 0.1% (v/v) formic acid were used as mobile
590 phase solvents with a flow rate of 12 mL/min. Chromatographic separation was achieved using
591 the following linear gradient (with percentages indicating levels of acetonitrile with formic acid):
592 10%, 3 column volumes (CV); 10% to 20%, 3 CV; 20% to 50%, 25 CV; 50% to 95%, 5 CV; 95%,
593 10 CV. Fractions were assayed by LC-MS; fractions containing pure 3-oxotomatidine were
594 combined and evaporated to dryness.

595 Tomatidine sulfate

596 Tomatidine sulfate synthesis was adapted from previous reports for the sulfation of dietary
597 phenolics[64]. Tomatidine hydrochloride was dissolved in pyridine and combined with one molar
598 equivalent of sulfur trioxide pyridine complex. The mixture was sparged with argon and stirred at
599 65°C for 24 hours. The reaction was quenched with one volume of water and the organic
600 solvent evaporated. The crude reaction mixture was analyzed by LC-MS for retention time
601 match and MS/MS match to the mass feature in biological samples.

602 Dihydrosolanidine

603 Dihydrosolanidine was synthesized from solanidine (Carbosynth) by hydrogenation mediated by
604 a palladium on carbon catalyst. Solanidine was dissolved in ethanol and one mass equivalent of
605 palladium of carbon was added with stirring. Hydrogen gas was bubbled through the mixture for
606 6 hours and the reaction was filtered to remove catalyst. The crude reaction mixture was
607 analyzed by LC-MS for retention time match and MS/MS match to the sample mass feature.

608

609 **Human urine from colectomy patients**

610 Urine samples were collected from 12 patients with total colectomies (6 male and 6 female) and
611 17 patients with intact colons with no known gastrointestinal disease and no antibiotic use for

612 one month pre-collection (11 male and 6 female)[24]. Donors did not receive specified dietary
613 regimens or supplements.

614 Urine samples were centrifuged at 12,000 *g* for 10 minutes and then analyzed by LC-MS as
615 described below. Sample creatinine levels were measured using a colorimetric creatinine assay
616 kit (Abcam) and normalization factors were calculated using the Cockcroft-Gault equation[65]. Ion
617 counts for metabolites of interest were multiplied by the normalization factor to enable
618 comparison in compound abundance between samples.

619

620 **Anaerobic culturing**

621 Work with fecal samples and individual commensal strains was performed under anaerobic
622 conditions using an anaerobic chamber (Coy, 10% CO_2, 5% H_2). To maintain a reducing
623 environment for fecal bacteria during sample collection and handling, mouse and human feces
624 were suspended in pre-reduced transport medium[26]. Transport medium contained, per L: 0.2 g
625 KCl, 0.1 g $CaCl_2$, 0.1 g $MgCl_2$, 0.2 g KH_2PO_4, 1.15 g Na_2HPO_4, 3 g NaCl, 0.1 g uric acid, 0.1 g
626 glutathione. Human fecal samples were cultured in standard amino acid complete minimal
627 medium (SAAC), prepared as described by Dodd *et al*[66]. Human commensal type strains were
628 grown on either Brain Heart Infusion (Teknova) agar plates supplemented with 5 µg/mL hemin
629 and 0.5 µg/mL menadione (BHIS) or Columbia agar plates supplemented with 10% sheep blood
630 (Col-B). Liquid cultures were grown in Mega medium, a rich medium adapted from Han *et al*[67];
631 for our use, Mega medium was modified to exclude soluble starch and Tween 80 for combability
632 with downstream LC-MS analysis.

633

634 ***Ex vivo* steroidal alkaloid metabolism by mouse feces**

635 To assay for steroidal glycoalkaloid metabolism by murine fecal bacteria, freshly collected fecal
636 pellets were suspended at 2% w/v in pre-reduced transport medium and then vortexed until
637 homogenized. Larger particulates were allowed to settle, and the slurry was transferred to a
638 new tube. An equal volume of transport medium containing 40 µM tomatine was added to the
639 2% w/v fecal slurry, resulting in a final incubation of 1% w/v feces with 20 µM tomatine. Samples
640 were incubated anaerobically for 36 hours at 37°C. Following incubation, two volumes of 3:1
641 MeCN:MeOH were added to extract metabolites and quench metabolism. Samples were

642 vortexed, centrifuged at 12,000 *g* for 10 minutes, and then supernatant was diluted and filtered
643 through a 0.45 µm PTFE filter for analysis by LC-MS, as described below.

644

645 ***Ex vivo* human stool metabolism**

646 De-identified stool samples from human donors were collected as part of the RAMP study
647 (Rejuvenating the Aging Microbiota with Prebiotics, clinical trial ID: NCT03690999)[25]. This
648 cohort was comprised of 89 individuals (49 female and 40 male) ranging from 60 years to 83.9
649 years. A subset of feces samples from thirty donors prior to any dietary intervention were
650 randomly selected and assayed for SGA metabolism. Samples were stored at -20°C in donor's
651 home freezers until they were transferred to the research laboratory and stored at -80°C until
652 use. Frozen samples were transferred into an anaerobic chamber, suspended at 10% w/v in
653 pre-reduced transport medium with 20% glycerol, vortexed for 2 minutes to homogenize, and
654 then allowed to settle. The stool slurry was aliquoted into cryotubes, flash-frozen in liquid
655 nitrogen, and stored at -80°C until use. For use in metabolism assays, frozen stool
656 resuspensions were thawed, diluted to 1% v/w in pre-reduced transport medium, and combined
657 in 96 well plate format with an equal volume of 2x SAAC containing 40 µM of steroidal alkaloid
658 substrate. Each reaction contained final concentrations of 0.5% w/v stool sample, 1x SAAC, and
659 20 µM steroidal alkaloid substrate. Each combination of stool sample and substrate was
660 prepared in two sets of triplicates; one set was incubated anaerobically at 37°C for 48 hours
661 while another set was immediately frozen in liquid nitrogen as an unmetabolized control and
662 stored at -80°C. Following incubation for 48 hours, the other set of reactions was also frozen in
663 liquid nitrogen and stored at -80°C.

664 To mitigate effects from differential evaporation between wells, samples were lyophilized to
665 dryness in 96 well plates and then resuspended in three volumes of 2:1:1 MeCN:MeOH:H_2O.
666 Plates were vortexed and sonicated for 5 minutes to resuspend, and then stored at -80°C
667 overnight to precipitate any proteins. Samples were centrifuged at 3,000 *g* for 10 minutes,
668 diluted in resuspension solvent, and then filtered through a 0.45 µm PTFE filter for analysis by
669 LC-MS, as described below.

670

671

672

673 **Human commensal type strain culturing and metabolism**

674 Human commensal type strains were streaked from glycerol stocks onto Columbia blood agar
675 plates and incubated anaerobically at 37°C for about 2 days. Single colonies were inoculated
676 into Mega medium and grown anaerobically at 37°C. After 2 days growth, strains were
677 subcultured into fresh Mega medium and further incubated for 48 hours. Individual cultures were
678 pelleted by centrifugation at 6000 *g* for 10 minutes, and then resuspended in pre-reduced PBS.
679 Resuspended cultures were used to inoculate modified Mega medium (without Tween and
680 soluble starch) supplemented with 25 μM steroidal alkaloid substrate and grown anaerobically at
681 37°C for 2 days. After incubation, cultures were flash-frozen in liquid nitrogen and lyophilized to
682 dryness to mitigate the effects of evaporation. Dried reactions were resuspended in three times
683 the original reaction volume with 2:1:1 MeCN:MeOH:H_2O, vortexed and sonicated to resuspend,
684 and then frozen at -80°C. Prior to analysis by LC-MS, samples were centrifuged at 4000 *g* for 15
685 minutes to remove particulates, diluted, and then filtered through a 0.45 μm PTFE filter.

686

687 **Phylogenetic analysis of human commensal type strains**

688 Taxonomic classifications of the human commensal type strains were determined using the
689 GTDBtk v.1.6.0 classify workflow which uses 120 marker genes from bacterial whole genome
690 sequences to place strains of interest in a GTDBtk reference tree (release202)[68]. Bacterial
691 genomes were obtained from the NIH Human Microbiome Project[69]. Trees were visualized
692 using Geneious.

693

694 **Metabolism of steroidal alkaloids by commensal cocultures**

695 *Bacteroides* and *Roseburia* strains were streaked from glycerol stocks onto BHIS plates and
696 incubated anaerobically at 37°C for one day. Single colonies were inoculated into pre-reduced
697 Mega medium and grown anaerobically at 37°C for about one day. Liquid cultures were
698 subcultured once more into Mega medium and allowed to grow anaerobically for a day. An
699 equal volume of each culture was combined, pelleted by centrifugation at 6,000 *g* for 10
700 minutes, and resuspended in one volume of fresh Mega medium supplemented with 20 μM
701 tomatine substrate. Cocultures were incubated anaerobically at 37°C for three days. Samples
702 were frozen at -80°C and lyophilized to dryness. Dried samples were then extracted with three

703 volumes of 2:1:1 MeCN:MeOH:H_2O, vortexed and sonicated to resuspend, and centrifuged at
704 4000 *g* for 15 minutes and filtered through a 0.45 µm PTFE filter prior to LC-MS analysis.

705

706 ***In vitro* cell viability assays**

707 The human intestinal epithelial cell line Caco-2 (ATCC, provided by Sarah Heilshorn, Stanford)
708 and used between passages 5 to 15. Cells were grown and maintained in DMEM (ATCC)
709 supplemented with 10% fetal bovine serum, 1% nonessential amino acids, 100 U/mL penicillin,
710 and 100 µg/mL streptomycin at 37°C in 5% CO_2. Cells were seeded into 96 well plates at a
711 density of 10,000 cells per well and incubated for 17 hours for cells to adhere. Cells were then
712 treated with varying concentrations of steroidal alkaloid compounds dissolved in solvent vehicle.
713 The total amount of vehicle added to each well was normalized to 0.4% v/v. As a nontreated
714 control, cells were treated with vehicle alone. Cells were incubated with compound at 37°C for
715 24 hours, after which cell viability was determined using the CellTiter-Glo Luminescent Cell
716 Viability Assay (Promega). All treatments were performed in triplicate and repeated in three
717 separate experiments.

718

719 **Caco-2 permeability assay**

720 Transport of steroidal alkaloid compounds *in vitro* were determined using differentiated Caco-2
721 cells as a model monolayer[27]. Cells were seeded into 12 well plates fitted with 0.4 µm
722 polycarbonate Transwell inserts (Corning) at a density of 300,000 cells per insert. The apical
723 compartment above the insert was filled with 0.5 mL of medium and the basolateral
724 compartment below the insert was filled with 1.5 mL of medium. Medium was refreshed on both
725 the apical and basolateral sides every 2 to 3 days for 21 days for monolayer formation. After 21
726 days, cells were rinsed with serum free DMEM supplemented with 1% nonessential amino
727 acids, 100 U/mL penicillin, and 100 µg/mL streptomycin. The apical compartment was filled with
728 serum-free DMEM additionally supplemented with nontoxic concentrations of steroidal alkaloid
729 compounds, as determined by viability assays described above (solanine: 10 µM, chaconine: 3
730 µM, solanidine: 10 µM). A subset of wells was treated with vehicle only as a control. The
731 basolateral compartment was filled with serum-free DMEM supplemented with 4% bovine serum
732 albumin (BSA) to mimic physiological protein concentrations on either side of the intestinal
733 epithelium. After 17 hours of incubation with steroidal alkaloid compounds, medium was

734 collected from both the apical and basolateral components. An aliquot of medium was assayed
735 for extracellular LDH using the LDH-Glo Cytotoxicity Assay (Promega) to ensure that cell
736 monolayers were not compromised by compound treatment. All compound-treated wells
737 showed similar LDH levels to vehicle only treatment, indicating that compound treatments at the
738 selected concentrations did not impact cell viability. The remainder of the medium collected was
739 assayed for steroidal alkaloid content using LC-MS. To prepare medium for analysis, samples
740 were diluted with nine volumes of 3:1 MeCN:MeOH, kept at -20°C overnight to precipitate
741 proteins, centrifuged at 10,000 *g* for 10 minutes, and filtered through a 0.45 µm PTFE filter.

742

743 **Cholinesterase activity assay**

744 Acetylcholinesterase (AChE) and butyrylcholinesterase (BChE) activities were measured using
745 Ellman's method, adapted to a 96-well format[35]. For acetylcholinesterase activity, 5 ng of
746 recombinant human AChE (Sigma) or 30 µg of tissue lysate was incubated with steroidal
747 alkaloid compound or at room temperature for 30 minutes in 50 mM Tris pH 8.0 in a total
748 volume of 90 µL. To initiate reactions, 5 µL of 10 mM acetylthiocholine iodide and 5 µL of 10
749 mM 5,5'-dithiobis-(2-nitrobenzoic acid) (DTNB) were added to each well and absorbance at 405
750 nm was measured over the course of 30 minutes. BChE activity was analogously measured
751 using 5 ng of recombinant human BChE (R&D Systems) and butyrylthiocholine iodide. Enzyme
752 activity was quantified as the linear slope of absorbance over time. Relative inhibition by
753 steroidal alkaloid compounds was quantified by normalization to enzyme activity in the presence
754 of vehicle.

755

756 **Colon lysate preparation**

757 Normal human colon tissue from three de-identified human donors was obtained from the
758 Stanford Tissue Bank. About 100 mg of tissue was homogenized in 2 mL of tissue lysis buffer
759 (50 mM Tris pH 8, 150 mM sodium chloride, 0.5% Triton X-100, 10 µg/mL leupeptin, 10 µg/mL
760 aprotinin, 20 µM pepstatin, and 2.5 mM benzamidine hydrochloride) using a gentleMACs Tissue
761 Dissociator (Miltenyi). Homogenized samples were centrifuged at 2,000 *g* for 5 minutes at 4°C
762 to collect lysate, transferred to new centrifuge tubes, and centrifuged at 9,000 *g* for 20 minutes
763 at 4°C to pellet cell debris.

764 To prepare protein lysates from Caco-2 intestinal epithelial cells, cells were maintained as
765 described above. A confluent 10 cm plate was rinsed three times with cold PBS, and then lysed
766 by adding tissue lysis buffer and incubating with rocking at 4°C for 20 minutes. Lysate was
767 collected and centrifuged at 9,000 g at 4°C for 20 minutes to remove cell debris.

768 To the resulting supernatants from human tissue and Caco-2 cells, glycerol was added to the
769 resulting supernatant for a final concentration of 20%. Protein concentrations in lysates were
770 estimated using BSA standards and a detergent-compatible Bradford assay (Abcam). Lysates
771 were aliquoted, flash-frozen in liquid nitrogen, and stored at -80°C until analysis by Ellman's
772 assay as described above. To assay the contributions of AChE to acetylthiocholine hydrolysis in
773 these homogenates, BChE-specific inhibitor iso-OMPA was added to homogenates at a
774 concentration of 500 μM and incubated at room temperature for 30 minutes before the assay
775 was initiated with acetylthiocholine and DTNB.

776

777 **Acetylcholinesterase inhibition by human stool samples**

778 A subset of eleven of the previously assayed de-identified human stool samples was selected
779 for their differences in solanine metabolism, including samples that did not appear to metabolize
780 solanine (02, 17, 22, 28), samples that deglycosylated solanine (07, 13, 23, 30), and samples
781 that appeared to partially deglycosylate solanine by removing a glucose moiety from the glycone
782 (08, 15, 16). *Ex vivo* incubations with 20 μM solanine or DMSO vehicle were prepared as
783 described above for each of the donor samples. For compatibility with Ellman's assay, we
784 minimized the presence of free thiols in the assay medium; these *ex vivo* stool incubations were
785 performed in pre-reduced SAAC minimal medium formulated without cysteine. Samples were
786 incubated anaerobically at 37°C for 48 hours, after which an aliquot was removed for LC-MS
787 analysis. This aliquot was diluted in 3:1 MeCN:MeOH to precipitate proteins, centrifuged at
788 12,000 *g* for 10 minutes, diluted in 2:1:1 MeCN:MeOH:H_2O, and then filtered through a 0.45 μm
789 PTFE filter. The remainder of the samples was spun down at 12,000 *g* for 20 minutes and the
790 resulting supernatant used to inhibit recombinant human AChE as described above, with a few
791 adaptations. These AChE assays were performed in spent supernatant from human stool
792 cultures instead of 50 mM Tris pH 8. Metabolism by stool samples appeared to lower media pH;
793 to adjust the assay pH to levels amenable to AChE activity and DTNB-thiol conjugation, equal
794 volumes of sodium hydroxide was added to samples at a final concentration of 6 mM. Sodium
795 hydroxide was not added to media-only controls (i.e. sterile).

796 **LC-MS**

797 *Ad libitum* fresh tomato feeding and pure tomatine feeding

798 Mouse serum and tissues resulting from fresh tomato supplementation and pure tomatine
799 feeding were analyzed on an Agilent 1260 Infinity II HPLC using both reversed-phase liquid
800 chromatography (LC) and normal phase LC. Reversed-phase LC was conducted using a
801 Gemini NX-C18 2x100 mm, 5 µm column (Phenomenex) at 40°C. Mobile phase solvents were
802 water with 0.1% (v/v) formic acid and acetonitrile with 0.1% (v/v) formic acid at a flow rate of 0.4
803 mL/min. A volume of 3 µL of sample was injected. Chromatographic separation was achieved
804 using the following linear gradient (with percentages indicating the levels of acetonitrile with
805 formic acid): 3% to 97%, 20 minutes; 97%, 5 minutes; 97% to 3%, 1 minute; 3%, 5 minutes.
806 Normal phase liquid chromatography was conducted using a Poroshell 120 HILIC-Z, 2.1x100
807 mm, 2.7 µm column (Agilent) at 40°C. Mobile phase solvents were 10 mM ammonium formate
808 supplemented with 0.1% formic acid and 90% acetonitrile with 10 mM ammonium formate
809 supplemented with 0.1% formic acid at a flow rate of 0.25 mL/ min. A volume of 2 µL of sample
810 was injected. Chromatographic separation was achieved using the following linear gradient (with
811 percentages indicating the levels of acetonitrile-containing mobile phase): 100% to 60%, 15
812 minutes; 60%, 2 minutes; 60% to 100%, 1 minute; 100%, 8 minutes. For both types of
813 chromatography, coupled mass spectrometry (MS) data was collected with an Agilent 6545
814 quadrupole time-of-flight (qTOF) ESI mass spectrometer in positive polarity. Parameters for the
815 6545 qTOF MS were as follows: mass range: 50-1700 m/z, gas temperature: 250°C, nebulizer:
816 10 psi, drying gas flow rate: 12 L/min, sheath gas temperature: 300°C, sheath gas flow rate: 12
817 L/min, fragmentor: 100 V, skimmer: 50 V.

818 Human urine

819 Urine from human colectomy patients and donors with intact colons were chromatographically
820 separated on an Agilent 1260 Infinity II HPLC using both reversed-phase LC. LC was conducted
821 using a SB-C18 3.0x100 mm, 1.8 µm column (Agilent) at 40°C. Mobile phase solvents were
822 water with 0.1% (v/v) formic acid and acetonitrile with 0.1% (v/v) formic acid at a flow rate of 0.4
823 mL/min. A volume of 5 µL of undiluted sample was injected. Chromatographic separation was
824 achieved using the following linear gradient (with percentages indicating the levels of acetonitrile
825 with formic acid): 3% to 97%, 20 minutes; 97%, 4 minutes; 97% to 3%, 1 minute; 3%, 4 minutes.
826 Coupled mass spectrometry (MS) data was collected with an Agilent 6545 quadrupole time-of-
827 flight (qTOF) ESI mass spectrometer in positive polarity. Parameters for the 6545 qTOF MS
828 were as follows: mass range: 50-1700 m/z, gas temperature: 250°C, nebulizer: 60 psi, drying

829 gas flow rate: 6 L/min, sheath gas temperature: 250°C, sheath gas flow rate: 11 L/min,
830 fragmentor: 140 V, skimmer: 65 V.

831 All other studies

832 Samples from all other studies were separated on an Agilent 1290 Infinity II HPLC using
833 reversed phase (LC). Chromatography for mouse serum and tissue samples and human liver
834 enzyme incubations was performed using a Zorbax RRHT Eclipse Plus C18, 2.1x100 mm, 1.8
835 µm column (Agilent) at 40°C. Mobile phase solvents were water with 0.1% (v/v) formic acid and
836 acetonitrile with 0.1% (v/v) formic acid at a flow rate of 0.4 mL/min. Chromatographic separation
837 was achieved using the following linear gradient (with percentages indicating the levels of
838 acetonitrile with formic acid): 3% to 97%, 20 minutes; 97%, 5 minutes; 97% to 3%, 1 minute;
839 3%, 5 minutes. Chromatography for human stool incubations, commensal type strain cultures,
840 bacterial cocultures, and Caco-2 monolayer transport studies was performed using a Zorbax
841 RRHT Eclipse Plus C18, 2.1x50 mm, 1.8 µm column (Agilent) at 40°C. Mobile phase solvents
842 were water with 0.1% (v/v) formic acid and acetonitrile with 0.1% (v/v) formic acid at a flow rate
843 of 0.6 mL/min. Chromatographic separation was achieved using the following linear gradient
844 (with percentages indicating the levels of acetonitrile with formic acid): 3% to 60%: 6 minutes,
845 60% to 95%: 0.1 minutes, 95%: 1.5 minutes, 95% to 3%: 0.1 minutes, 3%: 1 minute. For all
846 samples, a volume of 1 µL of sample was injected. MS data was collected using an Agilent 6546
847 qTOF ESI mass spectrometer in positive polarity. Parameters for the 6546 qTOF MS were as
848 follows: mass range: 50-1700 m/z, gas temperature: 325°C, nebulizer: 35 psi, drying gas flow
849 rate: 10 L/min, sheath gas temperature: 400°C, sheath gas flow rate: 12 L/min, fragmentor: 140
850 V, skimmer: 45 V.

851 Data analysis: untargeted metabolomics

852 Untargeted metabolomics was performed using XCMS Online[70]. Mass features were detected
853 using the centWave algorithm, with the following parameters:

854 Maximal tolerated m/z deviation: 30 ppm
855 Chromatographic peak width [min, max]: [10 seconds, 60 seconds]
856 Signal to noise threshold: 10
857 Minimum m/z difference in features with overlapping retention times: 0.01

858 Retention time correction was performed using the obiwarp method, with a step size of m/z 0.5.
859 Peak alignment was performed with bandwidth of 3 seconds and minimum fraction (minfrac) of
860 samples necessary for a valid group of 0.5.

861 From the table of mass features generated by XCMS Online, filtering criteria were applied to
862 identify features present or differentially accumulating in certain treatment groups. The first
863 filtering criteria was retention time; all mass features that eluted before 1 minute were assumed
864 to not be retained on the column and therefore discarded. Feature peak areas that were
865 statistically significantly different between treatment groups were then identified by Student's t-
866 test ($p < 0.1$ for normal phase analysis and $p < 0.05$ for reverse phase analysis). Features that
867 were higher in the treatment group of interest (e.g. higher in the serum of tomato-fed mice than
868 in the serum of un-supplemented mice) were identified by fold change difference (ratio of
869 average peak areas between groups). Mass features above a threshold signal (peak height >
870 10^4) were then retained. Finally, putative parent ions were identified by retention time and peak
871 area clustering to remove adducts, potential fragment ions, dimers, and isotopologues.

872 Data analysis: semi-targeted analysis for steroidal alkaloids in complex samples
873 To search for compounds in human stool incubations containing steroidal alkaloid
874 substructures, one set of replicates was analyzed with a constant collision energy of 40V (for
875 tomatidine-derived compounds) or 60V (for solanidine- and solasodine-derived compounds).
876 Ions characteristic of tomatidine, solanidine, and solasodine fragmentation at these collision
877 energies were extracted; tomatidine-derived: $[M+H]^+$ 161.1325, solanidine-derived: $[M+H]^+$
878 98.0964, and solasodine-derived: $[M+H]^+$ 157.1012. To find the unfragmented mass features
879 that yielded these characteristic fragments, the same sample was run with a collision energy of
880 0V and mass features that accumulated at the retention time of interest after stool sample
881 incubation were identified for further characterization by MS/MS.

882 Data analysis: targeted analysis
883 Extracted ion chromatograms (EIC) were extracted from raw data files using MassHunter
884 Qualitative Data Analysis software and integrated using MassHunter Quantitative Data Analysis
885 software. EICs were extracted using a 20-40 ppm window centered on the exact m/z value
886 (**Supplemental Table 1**).

887

888 **Statistics**

889 Statistical analyses were performed using Prism 9 (GraphPad). Pairs of sample groups were
890 analyzed using two-sided Welch's t test to account for unequal variance. Multiple groups of
891 samples were analyzed using a one-way ANOVA with multiplicity-adjusted P values calculated
892 using Tukey's multiple comparison test. Gaussian distribution was assumed.

DATA AVAILABILITY

All data in this manuscript are available upon request. Any materials generated within this manuscript will be made available, as possible.

ACKNOWLEDGEMENTS

This work was supported by a USDA NIFA grant 2022-67017-36242 (to E.S.S.). C.S.L. was supported by a Bio-X Bowes Fellowship. We thank J.L. Sonnenburg (Stanford) and T.W. Meyer (Stanford) for generously providing human samples for analysis; M. Carter for assistance accessing human stool samples; J.Z. Long and J.T. Kim (Stanford) for helpful discussions and preliminary experiments; E.A. Schulman (Stanford) for assistance with preliminary experiments; A.G. Cheng (Stanford) for helpful discussions and sharing protocols; J. Arreola (Stanford) for assistance with strain growth; S. Jain (C.Z. Biohub) for assistance with phylogenetic analyses; D.L. Wengier (Stanford) for assistance with acquiring tomatoes; J.C.T. Liu (Stanford) for assistance with structural characterization and comments on this manuscript; J.E. Blum and S.P. Niehs for comments on this manuscript.

CONTRIBUTIONS

C.S.L. and E.S.S designed experiments and analyzed data. C.S.L performed all experiments in the manuscript. M.I. and P.P.M. helped prepare human commensal strains. S.K.H. and M.J. assisted with mouse studies. J.R. assisted with human urine metabolomics analysis. C.S.L. wrote the paper with edits from E.S.S., M.A.F., and J.R.

DECLARATION OF INTERESTS

M.A.F. is a cofounder and director of Kelonia, a cofounder of Revolution Medicines, and a member of the scientific advisory boards of the Chan Zuckerberg Initiative and NGM Bio. The remaining authors declare no competing interests.

FIGURES

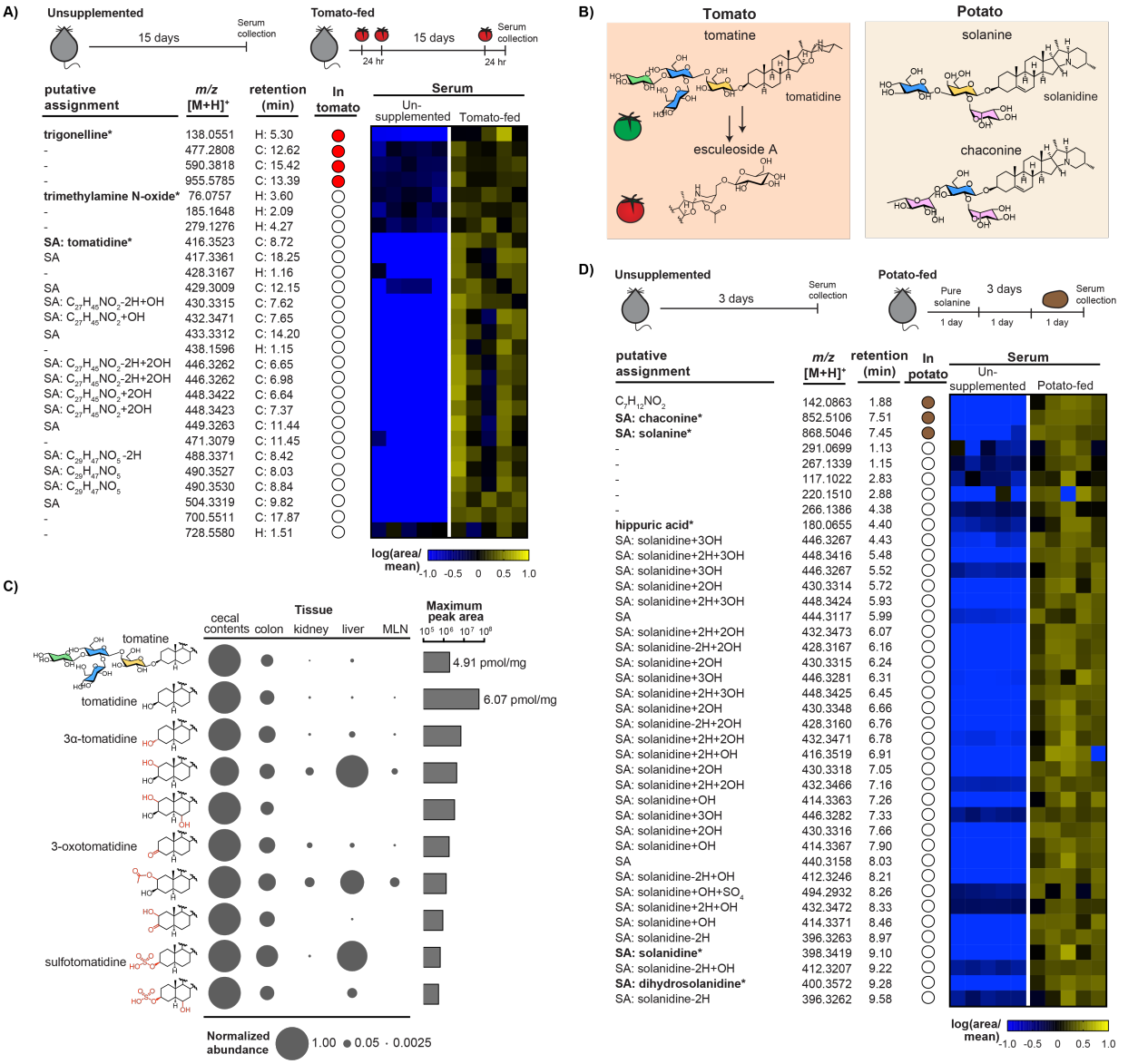

Figure 1. Major molecular inputs from dietary Solanums

A) Major mass features in mouse serum resulting from tomato intervention (schematic above) identified using untargeted metabolomics in positive ionization mode with reversed-phase (C: C18) and normal phase (H: HILIC) chromatography. Abundances for each individual (n=5 mice per treatment) are shown in the heat map as extracted ion chromatogram (EIC) peak areas normalized to the mean peak area for that mass feature across all individuals. Mass features also observed in the tomato supplement are marked with a red circle. Putative compound assignments are provided, with SA denoting putative steroidal alkaloid (SA) compounds. Assignments with an asterisk (*) have been confirmed by retention time and MS/MS matches to a chemical standard.

B) The major steroidal glycoalkaloids (SGAs) present in tomato and potato. Glycone monomers are colored by identity (blue: glucose, yellow: galactose, green: xylose, pink: rhamnose)

C) Accumulation of SGA-derived metabolites in mouse tissue following dietary intervention with purified tomatine. Metabolite abundances are represented by the mean EIC peak area for the compound (n=5 mice), normalized to the maximum peak area of that mass feature across different tissues. Peak areas were normalized by dry mass to enable comparison between different tissue types. The maximum EIC peak area across tissues is shown in the bars on the right, with molar quantities in pmol/mg dry weight shown for select compounds. Structures that have been characterized by comparison to a chemical standard or reproduced by *in vitro* enzyme reactions are named. Other structures are hypothesized based on *m/z* and MS/MS spectra; the positions of hydroxylations are not known. For molecules with multiple detected isomers, the most abundant isomer is shown.

D) Major mass features in mouse serum (n=5 mice per treatment) resulting from dietary potato intervention for 1 day, identified using untargeted metabolomics in positive ionization mode with C18 chromatography. Mass features also observed in the potato supplement are marked with a brown circle.

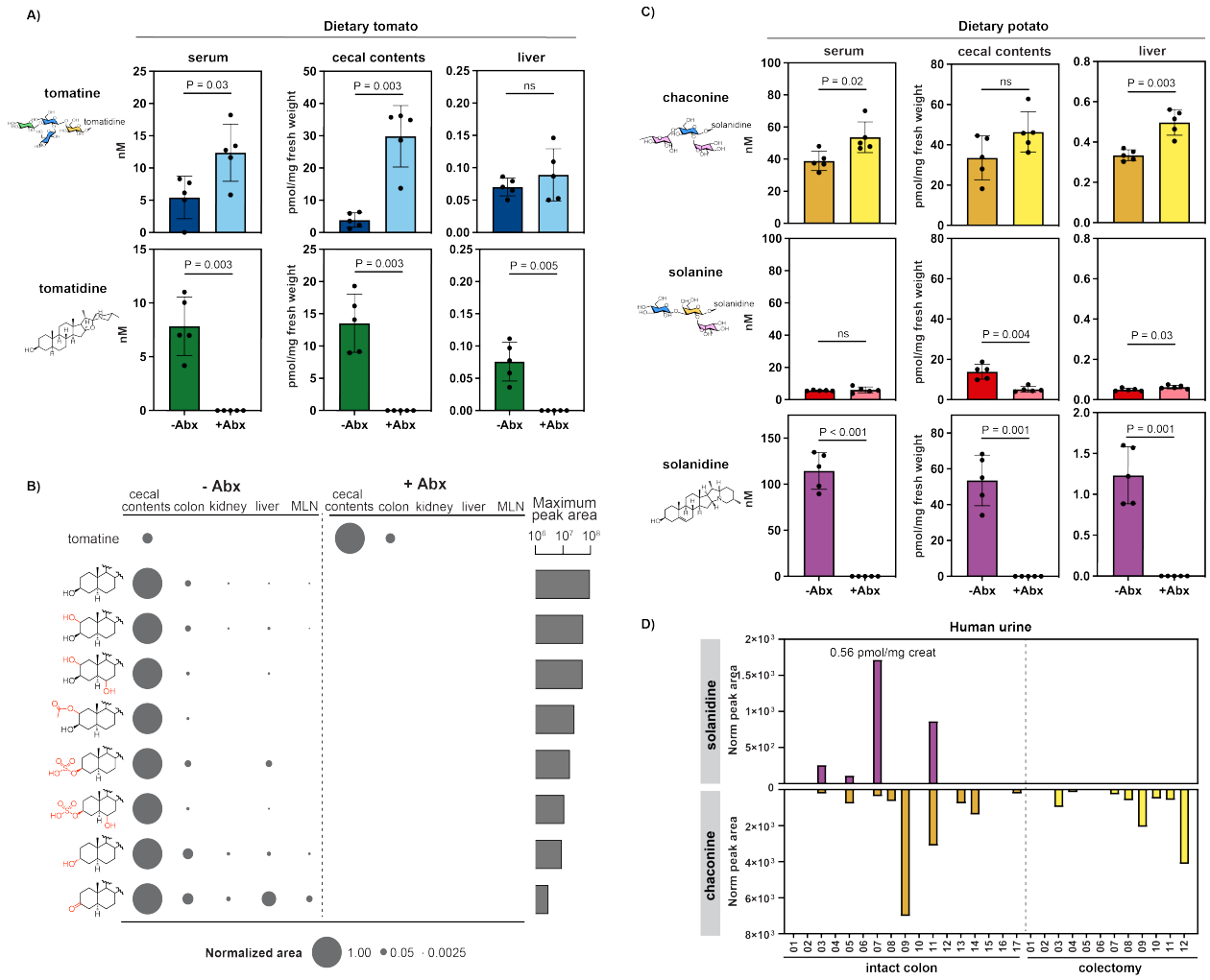

Figure 2. Gut microbiota gate host exposure to steroidal alkaloid aglycones

A) Tomatine and tomatidine concentrations in serum (nM), cecal contents (pmol/mg fresh weight), and liver (pmol/mg fresh weight) following a 10% tomato dietary intervention in C57BL/6J mice receiving antibiotics (Abx). Values shown are the mean±SD for each group, with individual replicates overlaid (n=5 mice per treatment). P values are determined using a two-sided Welch's T test. ns = not significant (P > 0.05).

B) Tomatine-derived metabolites in tissues following dietary intervention with 10% tomato diet in C57BL/6J mice receiving antibiotics. Abundances for each metabolite are normalized to the maximum EIC peak area across tissues shown in bars. Peak areas were normalized by sample dry mass to enable comparison between different tissue types. Values shown are the mean for each treatment group (n=5 mice per treatment). Structures as drawn are hypothesized based on *m/z* and MS/MS spectra; the position of hydroxylation is not known. For molecules with multiple detected isomers, the most abundant isomer is shown.

C) Chaconine, solanine, and solanidine concentrations in serum (nM), cecal contents (pmol/mg fresh weight), and liver (pmol/mg fresh weight) following a 5% potato dietary intervention in C57BL/6J mice receiving antibiotics. Values shown are the mean±SD for each treatment group, with individual replicates overlaid (n=5 mice per treatment). P values are determined using a two-sided Welch's T test. ns = not significant (P > 0.05).

968 D) Solanidine and chaconine in human urine from colectomy patients (n=12 donors) and donors
969 with intact colons (n=17 donors). Compound abundance is shown as EIC peak area
970 normalized to the creatinine content in that sample. Values shown are for individual donor
971 samples, with the molar concentration of solanidine in one intact colon sample shown in pmol
972 solanidine per mg creatinine.

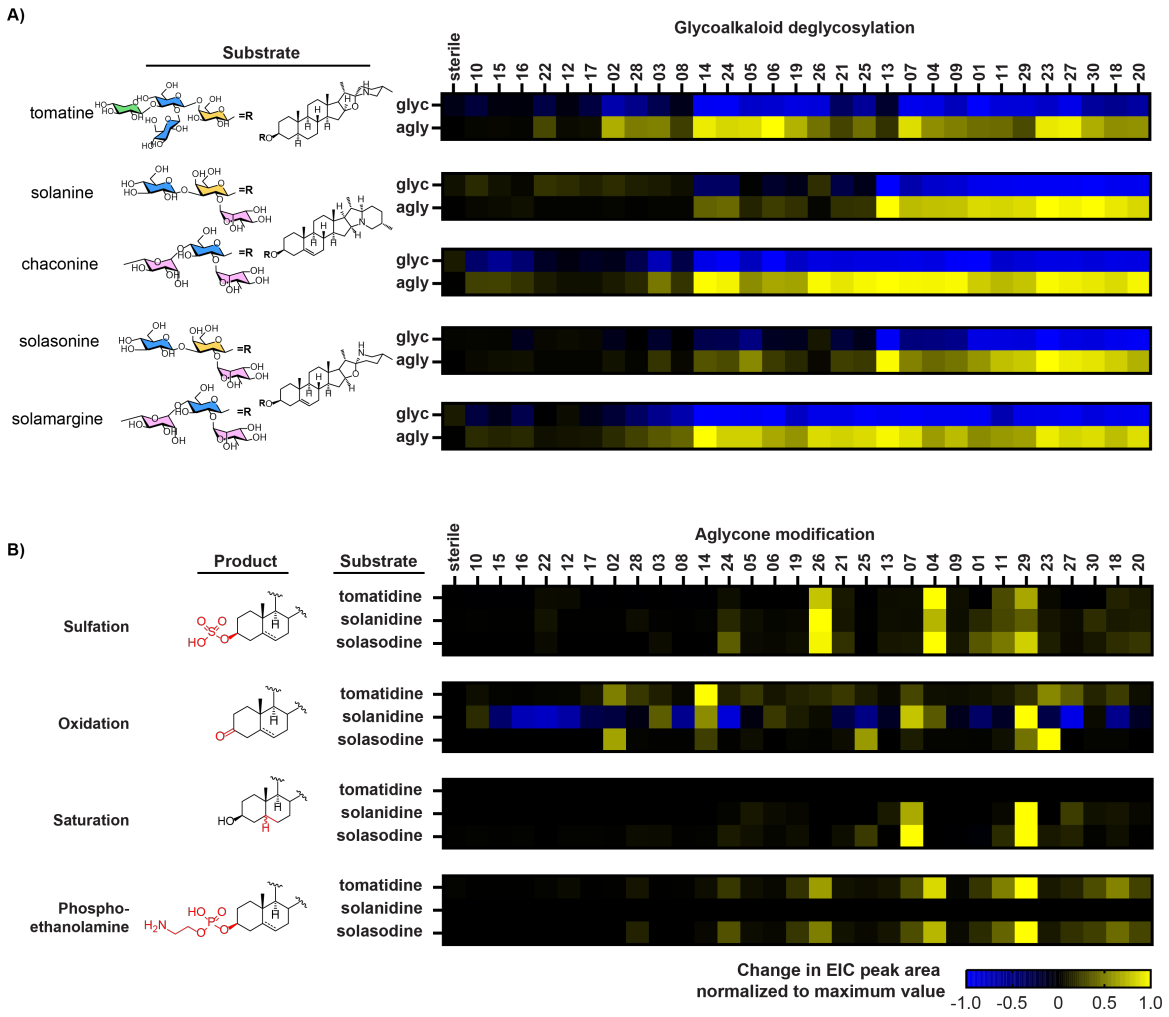

Figure 3. Inter-individual variation in *ex vivo* glycoalkaloid metabolism

A) Deglycosylation of tomato, potato, and eggplant SGAs by thirty human stool samples after incubation with substrate (25 μM) in SAAC minimal medium. Data shown are the change in mean EIC peak area of the tracked metabolite before and after 48 hours of incubation (n=3 replicate incubations per donor, substrate, and time point combination). Values are normalized to the maximum change registered across all donors. Total aglycone EIC peak areas were estimated as the sum of EIC peak areas of all tracked aglycones. A sterile sample without added human stool was included as a negative control.

B) Modification of tomato, potato, and eggplant steroidal alkaloid aglycones by human stool samples after incubation with substrate (25 μM) in SAAC minimal medium. Putative structures for modified aglycones are shown to the left. Donor samples are ordered according to deglycosylation activity shown in panel A. Data shown are the change in mean EIC peak area of the tracked metabolite before and after 48 hours of incubation (n=3 replicate incubations per donor, substrate, and time point combination).

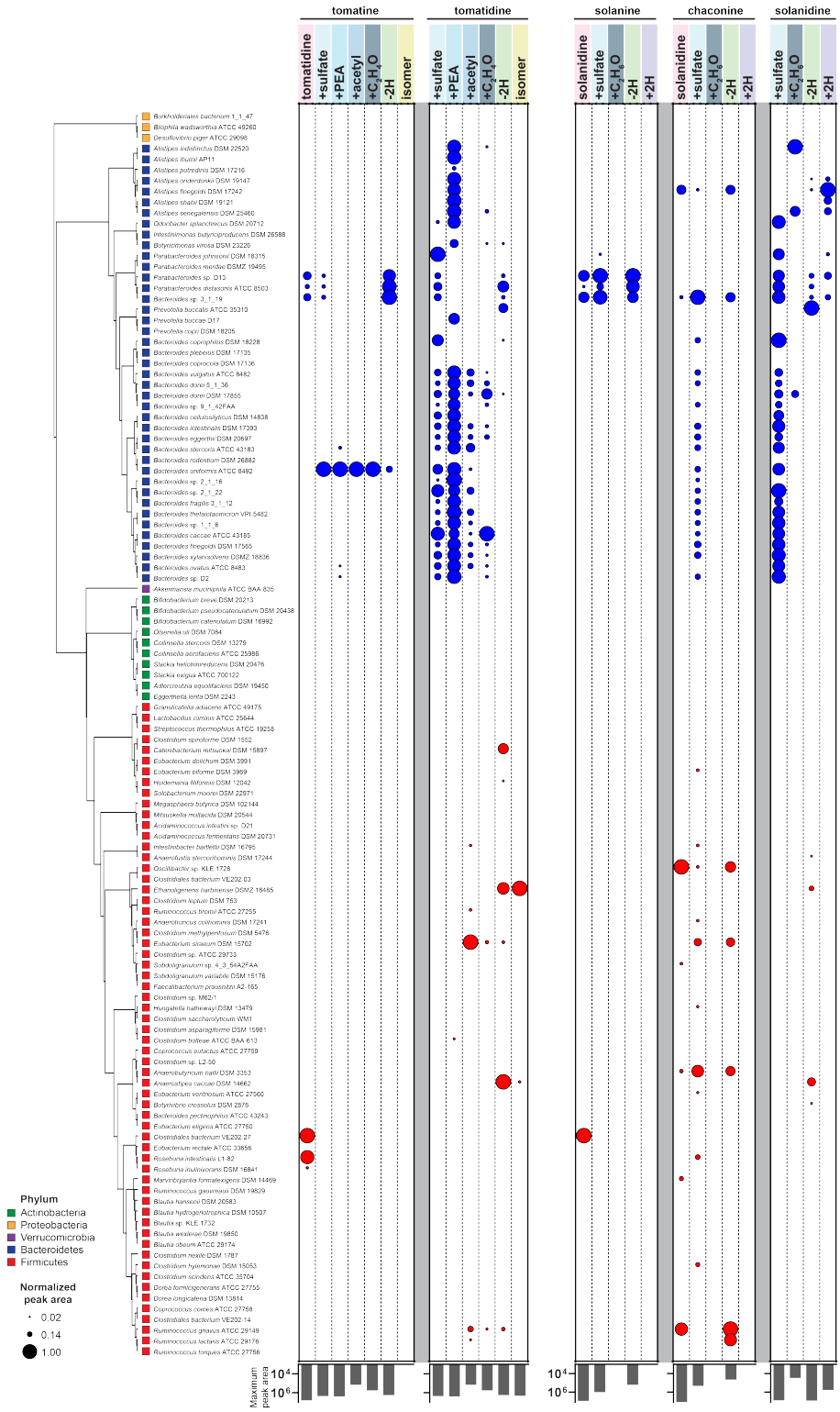

988

989 **Figure 4. SGA metabolism by human commensal type strains**

990 Metabolism of tomato and potato steroidal alkaloids by human commensal type strains after 48
991 hours of growth in rich Mega medium supplemented with steroidal alkaloid substrate (25 μM). A

992 phylogenetic tree of the surveyed strains is shown on the left, with boxes colored according to
993 phylum. Metabolite abundances are represented as the EIC peak area following incubation scaled
994 to the maximum EIC peak area of any sample incubated with the same substrate, values of which
995 are shown in grey bars at the bottom of the figure. Data are colored according to strain phylum.
996 Metabolite modifications: -2H: oxidation of 3OH, +2H: Δ5,6 saturation, +PEA:
997 phosphoethanolamine conjugation. Data shown are representative of two experiments.

998

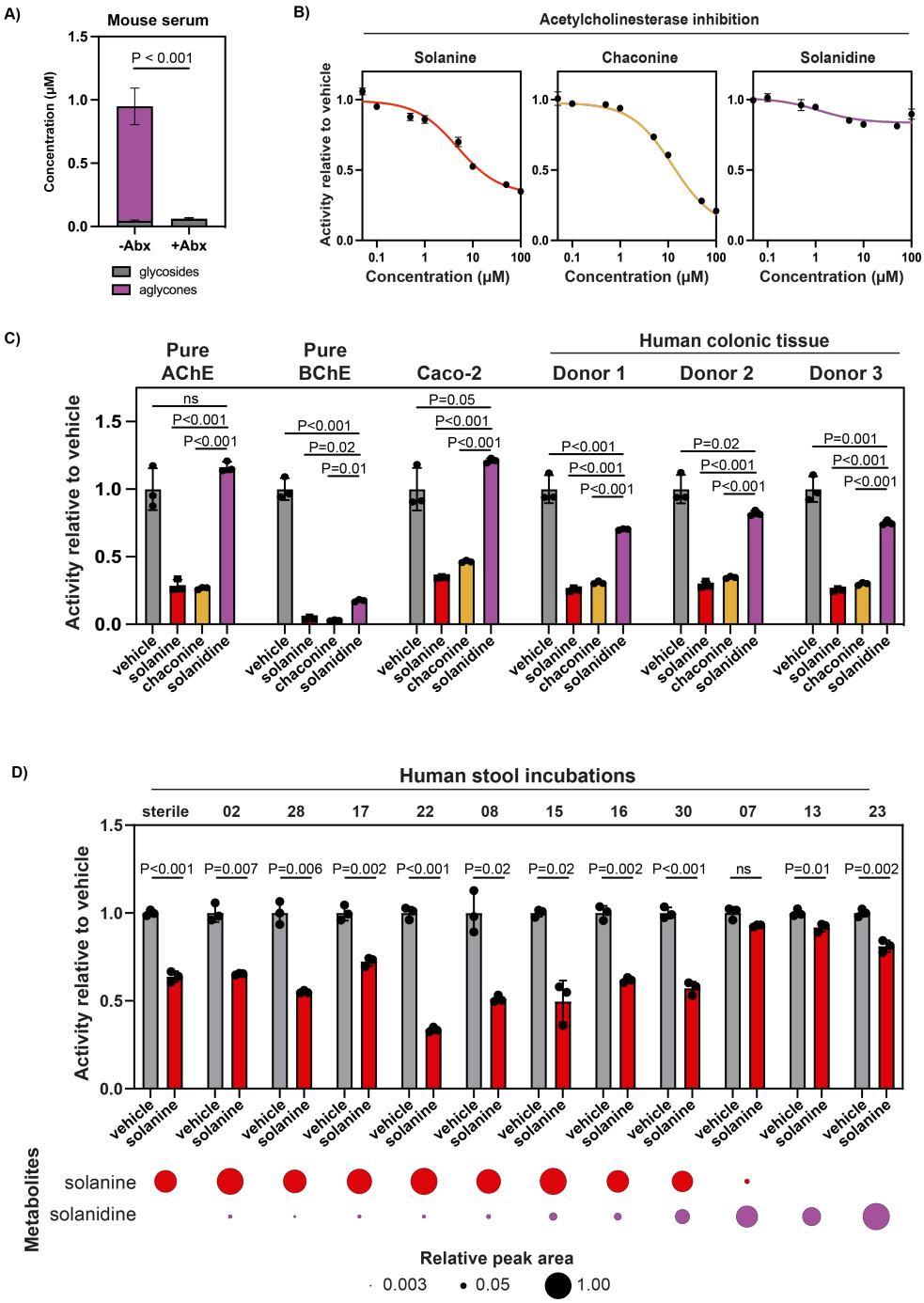

Figure 5. Microbiota-mediated SGA metabolism impacts compound bioavailability and bioactivity

A) Total steroidal alkaloid concentration in the serum of C57BL/6J mice fed potato-supplemented diet and treated with antibiotics. Aglycone concentrations were estimated using a solanidine standard curve. Data shown are the mean±SD (n=5 mice). P values were determined using a two-sided Welch's T test.

B) *In vitro* inhibition of recombinant human AChE activity by potato steroidal alkaloids. Data shown are normalized to AChE treated with vehicle only (DMSO for solanine, chaconine and

1008 ethanol for solanidine) with a total vehicle concentration of 1% for all treatments. Values
1009 shown are the mean±SD (n=3 assays per concentration). 5 ng of AChE was used in each
1010 reaction.

1011 C) *In vitro* inhibition of cholinesterase activity by 50 μM potato SAs in human protein
1012 homogenates from normal colonic tissue (n=3 donors) and Caco-2 colonic epithelial cells.
1013 Activity was normalized to the activity of the vehicle-treated sample. Values shown are the
1014 mean±SD of three replicate assays per homogenate. 5 ng each of recombinant human AChE
1015 and BChE were used for pure protein reactions, while 35 μg total protein was used for each
1016 homogenate. Multiplicity-adjusted P values were calculated using Tukey's multiple
1017 comparison tests.

1018 D) Inhibition of recombinant human AChE activity by spent media from human stool (n=11
1019 donors) incubated with 20 μM solanine in SAAC minimal medium. Activity was normalized to
1020 the activity of AChE treated with spent media from the same donor sample incubated with
1021 vehicle only. Values shown are the mean±SD of three AChE activity assays for each donor
1022 and compound combination. The relative abundances of select metabolites following
1023 incubation with solanine are shown below for each stool sample. Values shown are EIC peak
1024 areas normalized to the maximum peak area across all samples. P values were determined
1025 using a two-sided Welch's T test. Ns: not significant with P>0.05.

1026

1027 **REFERENCES**

1028 1. Murphy, M. M. *et al.* Phytonutrient Intake by Adults in the United States in Relation to Fruit
1029 and Vegetable Consumption. *J. Acad. Nutr. Diet.* **112**, 222–229 (2012).
1030 2. Tennant, D. R., Davidson, J. & Day, A. J. Phytonutrient intakes in relation to European fruit
1031 and vegetable consumption patterns observed in different food surveys. *Br. J. Nutr.* **112**,
1032 1214–1225 (2014).
1033 3. Butelli, E. *et al.* Enrichment of tomato fruit with health-promoting anthocyanins by
1034 expression of select transcription factors. *Nat. Biotechnol.* **26**, 1301–1308 (2008).
1035 4. Fahey, J. W., Zhang, Y. & Talalay, P. Broccoli sprouts: An exceptionally rich source of
1036 inducers of enzymes that protect against chemical carcinogens. *Proc. Natl. Acad. Sci. U. S.*
1037 *A.* **94**, 10367–10372 (1997).
1038 5. Turnbaugh, P. J. *et al.* An obesity-associated gut microbiome with increased capacity for
1039 energy harvest. *Nature* **444**, 1027–1031 (2006).
1040 6. Zimmermann, M., Zimmermann-Kogadeeva, M., Wegmann, R. & Goodman, A. L. Mapping
1041 human microbiome drug metabolism by gut bacteria and their genes. *Nature* **570**, 462–467
1042 (2019).
1043 7. Marcobal, A. *et al.* A metabolomic view of how the human gut microbiota impacts the host
1044 metabolome using humanized and gnotobiotic mice. *ISME J.* **7**, 1933–1943 (2013).
1045 8. Fuhrman, B. J. *et al.* Equol Status Modifies the Association of Soy Intake and
1046 Mammographic Density in a Sample of Postmenopausal Women. *Cancer Epidemiol.*
1047 *Biomarkers Prev.* **17**, 33–42 (2008).
1048 9. Koeth, R. A. *et al.* Intestinal microbiota metabolism of l-carnitine, a nutrient in red meat,
1049 promotes atherosclerosis. *Nat. Med.* **19**, 576–585 (2013).
1050 10. Economic Research Service (ERS), U.S. Department of Agriculture (USDA). Food
1051 Availability (Per Capita) Data System.
1052 11. Chaudhary, P., Sharma, A., Singh, B. & Nagpal, A. K. Bioactivities of phytochemicals
1053 present in tomato. *J. Food Sci. Technol.* **55**, 2833–2849 (2018).
1054 12. Schieber, A. & Saldaña, M. Potato Peels: A Source of Nutritionally and Pharmacologically
1055 Interesting Compounds – A Review. *Food* **3**, 23–29 (2009).
1056 13. Agarwal, S. & Rao, A. V. Tomato lycopene and low density lipoprotein oxidation: A human
1057 dietary intervention study. *Lipids* **33**, 981–984 (1998).
1058 14. Sesso, H. D., Liu, S., Gaziano, J. M. & Buring, J. E. Dietary Lycopene, Tomato-Based Food
1059 Products and Cardiovascular Disease in Women. *J. Nutr.* **133**, 2336–2341 (2003).
1060 15. Simó, C. & García-Cañas, V. Dietary bioactive ingredients to modulate the gut microbiota-
1061 derived metabolite TMAO. New opportunities for functional food development. *Food Funct.*
1062 **11**, 6745–6776 (2020).
1063 16. Zhu, W. *et al.* Gut Microbial Metabolite TMAO Enhances Platelet Hyperreactivity and
1064 Thrombosis Risk. *Cell* **165**, 111–124 (2016).
1065 17. Norred, W., Nishie, K. & Osman, S. Excretion, distribution and metabolic fate of 3H-alpha-
1066 chaconine. *Res. Commun. Chem. Pathol. Pharmacol.* **13**, (1976).
1067 18. Krupp, D., Doberstein, N., Shi, L. & Remer, T. Hippuric Acid in 24-Hour Urine Collections Is
1068 a Potential Biomarker for Fruit and Vegetable Consumption in Healthy Children and
1069 Adolescents,. *J. Nutr.* **142**, 1314–1320 (2012).
1070 19. Hövelmann, Y., Lewin, L., Steinert, K., Hübner, F. & Humpf, H. Mass Spectrometry–Based
1071 Analysis of Urinary Biomarkers for Dietary Tomato Intake. *Mol. Nutr. Food Res.* **64**,
1072 2000011 (2020).
1073 20. Cichon, M. J. *et al.* Plasma Metabolomics Reveals Steroidal Alkaloids as Novel Biomarkers
1074 of Tomato Intake in Mice. *Mol. Nutr. Food Res.* **61**, 1–9 (2017).

1075 21. Dzakovich, M. P. *et al.* Transcriptomics and Metabolomics Reveal Tomato Consumption
1076 Alters Hepatic Xenobiotic Metabolism and Induces Steroidal Alkaloid Metabolite
1077 Accumulation in Mice. *Mol. Nutr. Food Res.* **68**, 2300239 (2024).
1078 22. Cockburn, D. W. & Koropatkin, N. M. Polysaccharide Degradation by the Intestinal
1079 Microbiota and Its Influence on Human Health and Disease. *J. Mol. Biol.* **428**, 3230–3252
1080 (2016).
1081 23. Rakoff-Nahoum, S., Paglino, J., Eslami-Varzaneh, F., Edberg, S. & Medzhitov, R.
1082 Recognition of Commensal Microflora by Toll-Like Receptors Is Required for Intestinal
1083 Homeostasis. *Cell* **118**, 229–241 (2004).
1084 24. Mair, R. D., Sirich, T. L., Plummer, N. S. & Meyer, T. W. Characteristics of Colon-Derived
1085 Uremic Solutes. *Clin. J. Am. Soc. Nephrol.* **13**, 1398–1404 (2018).
1086 25. Carter, M. M. *et al. A Human Milk Oligosaccharide Alters the Microbiome, Circulating*
1087 *Hormones, Cytokines and Metabolites in a Randomized Controlled Trial of Older*
1088 *Individuals*. http://medrxiv.org/lookup/doi/10.1101/2023.08.18.23294085 (2023)
1089 doi:10.1101/2023.08.18.23294085.
1090 26. Cheng, A. G. *et al.* Design, construction, and in vivo augmentation of a complex gut
1091 microbiome. *Cell* **185**, 3617-3636.e19 (2022).
1092 27. Hubatsch, I., Ragnarsson, E. G. E. & Artursson, P. Determination of drug permeability and
1093 prediction of drug absorption in Caco-2 monolayers. *Nat. Protoc.* **2**, 2111–2119 (2007).
1094 28. Kuo, C. Y. *et al.* Tomatidine Attenuates Airway Hyperresponsiveness and Inflammation by
1095 Suppressing Th2 Cytokines in a Mouse Model of Asthma. *Mediators Inflamm.* **2017**, (2017).
1096 29. Shieh, J. M. *et al.* α-Tomatine Suppresses Invasion and Migration of Human Non-Small Cell
1097 Lung Cancer NCI-H460 Cells Through Inactivating FAK/PI3K/Akt Signaling Pathway and
1098 Reducing Binding Activity of NF-κB. *Cell Biochem. Biophys.* **60**, 297–310 (2011).
1099 30. Kúdelová, J. *et al.* Alpha-tomatine activates cell cycle checkpoints in the absence of DNA
1100 damage in human leukemic MOLT-4 cells. *J. Appl. Biomed.* **11**, 93–103 (2013).
1101 31. Friedman, M. *et al.* Tomatine-containing green tomato extracts inhibit growth of human
1102 breast, colon, liver, and stomach cancer cells. *J. Agric. Food Chem.* **57**, 5727–5733 (2009).
1103 32. Roddick, J. G. The acetylcholinesterase-inhibitory activity of steroidal glycoalkaloids and
1104 their aglycones. *Phytochemistry* **28**, 2631–2634 (1989).
1105 33. Nigg, H. N. *et al.* Inhibition of Human Plasma and Serum Butyrylcholinesterase (EC 3.1.1.8)
1106 by *α* -Chaconine and *α* -Solanine. *Toxicol. Sci.* **33**, 272–281 (1996).
1107 34. McMillan, M. & Thompson, J.C. An outbreak of suspected solanine poisoning in schoolboys:
1108 examination of criteria of solanine poisoning. *QJM Int. J. Med.* **48**, (1979).
1109 35. Ellman, G. L., Courtney, K. D., Andres, V. & Featherstone, R. M. A new and rapid
1110 colorimetric determination of acetylcholinesterase activity. *Biochem. Pharmacol.* **7**, 88–95
1111 (1961).
1112 36. Goyal, R. K. & Hirano, I. The Enteric Nervous System. *N. Engl. J. Med.* **334**, 1106–1115
1113 (1996).
1114 37. Kim, D. H. Gut microbiota-mediated pharmacokinetics of ginseng saponins. *J. Ginseng Res.*
1115 **42**, 255–263 (2018).
1116 38. Han, B. H., Park, M. H. & Han, Y. N. Degradation of ginseng saponins under mild acidic
1117 conditions. *Planta Med.* **44**, 146–149 (1982).
1118 39. Schneider, H., Schwiertz, A., Collins, M. D. & Blaut, M. Anaerobic transformation of
1119 quercetin-3-glucoside by bacteria from the human intestinal tract. *Arch. Microbiol.* **171**, 81–
1120 91 (1999).
1121 40. Day, A. J. *et al.* Deglycosylation of flavonoid and isoflavonoid glycosides by human small
1122 intestine and liver β-glucosidase activity. *FEBS Lett.* **436**, 71–75 (1998).
1123 41. Friedman, M., Kozukue, N. & Harden, L. A. Preparation and Characterization of Acid
1124 Hydrolysis Products of the Tomato Glycoalkaloid α-Tomatine. *J. Agric. Food Chem.* **46**,
1125 2096–2101 (1998).

42. Zhao, L. *et al.* Gut bacteria selectively promoted by dietary fibers alleviate type 2 diabetes. *Science* **359**, 1151–1156 (2018).
43. Rakoff-Nahoum, S., Coyne, M. J. & Comstock, L. E. An Ecological Network of Polysaccharide Utilization among Human Intestinal Symbionts. *Curr. Biol.* **24**, 40–49 (2014).
44. Wang, M. *et al.* Strain dropouts reveal interactions that govern the metabolic output of the gut microbiome. *Cell* **186**, 2839-2852.e21 (2023).
45. King, R. R. & McQueen, R. E. Transformations of Potato Glycoalkaloids by Rumen Microorganisms. *J. Agric. Food Chem.* **29**, 1101–1103 (1981).
46. Gérard, P. *et al. Bacteroides* sp. Strain D8, the First Cholesterol-Reducing Bacterium Isolated from Human Feces. *Appl. Environ. Microbiol.* **73**, 5742–5749 (2007).
47. Freier, T. A., Beitz, D. C., Li, L. & Hartman, P. A. Characterization of Eubacterium coprostanoligenes sp. nov., a Cholesterol-Reducing Anaerobe. *Int. J. Syst. Bacteriol.* **44**, 137–142 (1994).
48. Eyssen, H. J., Parmentier, G. G., Compernolle, F. C., De Pauw, G. & Piessens-Denef, M. Biohydrogenation of Sterols by *Eubacterium* ATCC 21,408— *Nova* Species. *Eur. J. Biochem.* **36**, 411–421 (1973).
49. Kenny, D. J. *et al.* Cholesterol Metabolism by Uncultured Human Gut Bacteria Influences Host Cholesterol Level. *Cell Host Microbe* **28**, 245-257.e6 (2020).
50. Ibach, B. & Haen, E. Acetylcholinesterase Inhibition in Alzheimers Disease. *Curr. Pharm. Des.* **10**, 231–251 (2004).
51. Almasieh, M., Zhou, Y., Kelly, M. E., Casanova, C. & Di Polo, A. Structural and functional neuroprotection in glaucoma: role of galantamine-mediated activation of muscarinic acetylcholine receptors. *Cell Death Dis.* **1**, e27–e27 (2010).
52. Andrew Luckey, Edward Livingston, & Yvette Tache. Mechanisms and Treatment of Postoperative Ileus. *Arch. Surg.* **138**, 206 (2003).
53. Slanina, P. Solanine (glycoalkaloids) in potatoes: Toxicological evaluation. *Food Chem. Toxicol.* **28**, 759–761 (1990).
54. Mensinga, T. T. *et al.* Potato glycoalkaloids and adverse effects in humans: An ascending dose study. *Regul. Toxicol. Pharmacol.* **41**, 66–72 (2005).
55. Patil, B. C., Sharma, R. P., Salunkhe, D. K. & Salunkhe, K. Evaluation of solanine toxicity. *Food Cosmet. Toxicol.* **10**, 395–398 (1972).
56. Yajima, T., Inoue, R., Matsumoto, M. & Yajima, M. Non-neuronal release of ACh plays a key role in secretory response to luminal propionate in rat colon. *J. Physiol.* **589**, 953–962 (2011).
57. Yu, H. *et al.* Acetylcholine acts through M3 muscarinic receptor to activate the EGFR signaling and promotes gastric cancer cell proliferation. *Sci. Rep.* **7**, 40802 (2017).
58. Billipp, T. E. *et al. Tuft Cell-Derived Acetylcholine Regulates Epithelial Fluid Secretion*. http://biorxiv.org/lookup/doi/10.1101/2023.03.17.533208 (2023) doi:10.1101/2023.03.17.533208.
59. Vizi, S. E., Bertaccini, G., Impicciatore, M. & Knoll, J. Evidence that Acetylcholine Released by Gastrin and Related Polypeptides Contributes to their Effect on Gastrointestinal Motility. *Gastroenterology* **64**, 268–277 (1973).
60. Dyle, M. C. *et al.* Systems-based discovery of tomatidine as a natural small molecule inhibitor of skeletal muscle atrophy. *J. Biol. Chem.* **289**, 14913–14924 (2014).
61. Hang, S. *et al.* Bile acid metabolites control TH17 and Treg cell differentiation. *Nature* **576**, 143–148 (2019).
62. Kuss, S. K. *et al.* Intestinal Microbiota Promote Enteric Virus Replication and Systemic Pathogenesis. *Science* **334**, 249–252 (2011).
63. Chagnon, F. *et al.* Unraveling the structure-activity relationship of tomatidine, a steroid alkaloid with unique antibiotic properties against persistent forms of Staphylococcus aureus. *Eur. J. Med. Chem.* **80**, 605–620 (2014).

1177 64. Almeida, A. F., Santos, C. N. & Ventura, M. R. Synthesis of New Sulfated and Glucuronated
1178 Metabolites of Dietary Phenolic Compounds Identified in Human Biological Samples. *J.*
1179 *Agric. Food Chem.* **65**, 6460–6466 (2017).
1180 65. Cockcroft, D. W. & Gault, H. Prediction of Creatinine Clearance from Serum Creatinine.
1181 *Nephron* **16**, 31–41 (1976).
1182 66. Dodd, D. *et al.* A gut bacterial pathway metabolizes aromatic amino acids into nine
1183 circulating metabolites. *Nature* **551**, 648–652 (2017).
1184 67. Han, S. *et al.* A metabolomics pipeline for the mechanistic interrogation of the gut
1185 microbiome. *Nature* **595**, (2021).
1186 68. Chaumeil, P. A., Mussig, A. J., Hugenholtz, P. & Parks, D. H. GTDB-Tk: A toolkit to classify
1187 genomes with the genome taxonomy database. *Bioinformatics* **36**, 1925–1927 (2020).
1188 69. The Human Microbiome Project Consortium. A framework for human microbiome research.
1189 *Nature* **486**, 215–221 (2012).
1190 70. Tautenhahn, R., Patti, G. J., Rinehart, D. & Siuzdak, G. XCMS Online: A Web-Based
1191 Platform to Process Untargeted Metabolomic Data. *Anal. Chem.* **84**, 5035–5039 (2012).
1192 71. Cahill, M. G., Caprioli, G., Vittori, S. & James, K. J. Elucidation of the mass fragmentation
1193 pathways of potato glycoalkaloids and aglycons using Orbitrap mass spectrometry. *J. Mass*
1194 *Spectrom.* **45**, 1019–1025 (2010).
1195 72. Caprioli, G., Cahill, M., Logrippo, S. & James, K. Elucidation of the mass fragmentation
1196 pathways of tomatidine and β1-hydroxytomatine using orbitrap mass spectrometry. *Nat.*
1197 *Prod. Commun.* **10**, 575–576 (2015).
1198 73. Falany, C. N., Wheeler, J., Tae Sung Oh & Falany, J. L. Steroid sulfation by expressed
1199 human cytosolic sulfotransferases. *J. Steroid Biochem. Mol. Biol.* **48**, 369–375 (1994).
1200 74. Yao, L. *et al.* A biosynthetic pathway for the selective sulfonation of steroidal metabolites by
1201 human gut bacteria. *Nat. Microbiol.* **7**, 1404–1418 (2022).
1202 75. Johnson, E. L. *et al.* Sphingolipids produced by gut bacteria enter host metabolic pathways
1203 impacting ceramide levels. *Nat. Commun.* **11**, 1–11 (2020).
1204 76. Panevska, A., Skočaj, M., Križaj, I., Maček, P. & Sepčić, K. Ceramide
1205 phosphoethanolamine, an enigmatic cellular membrane sphingolipid. *Biochim. Biophys.*
1206 *Acta - Biomembr.* **1861**, 1284–1292 (2019).
1207 77. Osbourn, A., Bowyer, P., Lunness, P., Clarke, B. & Daniels, M. Fungal Pathogens of Oat
1208 Detoxify Host Saponins. *Mpmi* **8**, (1995).
1209 78. Kaup, O., Gräfen, I., Zellermann, E. M., Eichenlaub, R. & Gartemann, K. H. Identification of
1210 a tomatinase in the tomato-pathogenic actinomycete Clavibacter michiganensis subsp.
1211 michiganensis NCPPB382. *Mol. Plant. Microbe Interact.* **18**, 1090–1098 (2005).
1212 79. Hennessy, R. C. *et al.* A Screening Method for the Isolation of Bacteria Capable of
1213 Degrading Toxic Steroidal Glycoalkaloids Present in Potato. *Front. Microbiol.* **9**, 2648
1214 (2018).
1215 80. Wang, W. *et al.* Glutamicibacter halophytocola-mediated host fitness of potato tuber moth
1216 on Solanaceae crops. *Pest Manag. Sci.* **78**, 3920–3930 (2022).
1217